

Measuring Fundamental Parameters of Substellar Objects. II: Masses and Radii

Subhanjoy Mohanty¹, Ray Jayawardhana², Gibor Basri³

ABSTRACT

We present mass and radius derivations for a sample of very young, mid- to late M, low-mass stellar and substellar objects in Upper Scorpius and Taurus. In a previous paper, we determined effective temperatures and surface gravities for these targets, from an analysis of their high-resolution optical spectra and comparisons to the latest synthetic spectra. We now derive extinctions, radii, masses and luminosities by combining our previous results with observed photometry, surface fluxes from the synthetic spectra and the known cluster distances. These are the first mass and radius estimates for young, very low mass bodies that are *independent* of theoretical evolutionary models (though our estimates do depend on spectral modeling). We find that for most of our sample, our derived mass-radius and mass-luminosity relationships are in very good agreement with the theoretical predictions. However, our results diverge from the evolutionary model values for the coolest, lowest-mass targets: our inferred radii and luminosities are significantly larger than predicted for these objects at the likely cluster ages, causing them to appear much younger than expected. We suggest that uncertainties in the evolutionary models - e.g., in the choice of initial conditions and/or treatment of interior convection - may be responsible for this discrepancy. Finally, two of our late-M objects (USco 128 and 130) appear to have masses close to the deuterium-fusion boundary (~ 9 – 14 Jupiters, within a factor of 2). This conclusion is primarily a consequence of their considerable faintness compared to other targets with similar extinction, spectral type, and temperature (difference of ~ 1 mag). Our result suggests that the faintest young late-M or cooler objects may be significantly lower in mass than current theoretical tracks indicate.

Subject headings: stars: low-mass, brown dwarfs – stars: pre-main sequence – stars: formation – stars: fundamental parameters – planetary systems – techniques: spectroscopic

¹Harvard-Smithsonian Center for Astrophysics, Cambridge, MA 02138. smohanty@cfa.harvard.edu

²Astronomy Department, University of Michigan, Ann Arbor, MI 48109. rayjay@umich.edu

³Astronomy Department, University of California, Berkeley, CA 94720. basri@soleil.berkeley.edu

1. Introduction

The last few years have witnessed a dramatic swelling in the ranks of objects at the bottom of the Main Sequence, and in the substellar regime beyond. Hundreds of ultra-low-mass stars and brown dwarfs have been uncovered, both in the field and in star-forming regions. Studies of young clusters even suggest the presence of isolated planetary mass objects (Zapatero et al. 2000; Lucas & Roche 2000). The existence and properties of all these low-mass bodies have profound implications for a host of issues, ranging from the dominant mechanisms for star and planet formation (Boss 2001; Reipurth & Clarke 2001; Bate et al. 2002; Padoan & Nordlund 2002), to the birthline and early evolution of low-mass objects (Hartmann 2003), to the shape of the initial mass function (Briceno et al. 2002). A reliable determination of mass is intrinsic to the ultimate resolution of these questions.

Presently, masses (and ages) are most widely inferred by comparing observables such as temperature and luminosity to the predictions of theoretical evolutionary tracks. However, these models remain largely unverified for very low masses. The simplest test is to derive dynamical masses for the components of binary (or higher-order) systems with known orbital parameters, and compare them to the theoretical values derived from other, directly observed quantities (e.g., L_{bol} and T_{eff}). Unfortunately, this is impeded for very low-mass stars and substellar objects by the current paucity of suitable multiple systems. In most known cases, one can either deduce dynamical masses but not theoretical ones (because the components are not directly detected), or vice versa (because the orbital parameters remain indeterminate). The one exception is HD 209458, in which both are available (Charbonneau et al. 2002). The comparison of theory to observations in this case does reveal some large uncertainties in the former, and underlines the usefulness of such tests (Baraffe et al. 2003; Burrows, Sudarsky & Hubbard 2003). However, it is not very illuminating as a general evaluation of the models: the proximity between the planetary companion and the star in this instance engenders special insolation effects, precluding an extension of the results to free-floating brown dwarfs and planetary mass objects (or to planets with larger orbital radii).

The situation is likely to improve in the near future, at least in the field - several promising systems with directly detected, probably substellar components have now come to light; dynamical masses should be obtained fairly soon (Close et al. 2002; Potter et al. 2002; Lane et al. 2001), allowing checks on the theoretical models for field brown dwarfs. In young clusters and star-forming regions, however, no suitable systems have emerged yet. This is especially troubling since even the identification of objects as substellar currently depends, at these early ages, on the theoretical tracks (empirical tests of substellarity that depend on Lithium detection or minimum Main Sequence temperature are largely inapplicable to very young objects). Moreover, the low-mass tracks are most uncertain precisely at such early

times (Baraffe et al. 2002), so testing them for young objects is particularly crucial.

To address this issue, we have developed a technique for calculating masses for young cluster objects from surface gravity measurements, independent of theoretical evolutionary models. The essential idea is simple: derive surface gravity and effective temperature (T_{eff}) by comparing the observed spectrum to the latest synthetic ones, then derive radius (and extinction) by combining the observed photometry and known cluster distance with the surface fluxes predicted by the synthetic spectra (for the inferred T_{eff} and gravity), and finally derive mass by combining radius and gravity. The sticking point, of course, is the derivation of sufficiently accurate surface gravities from the spectra, which has long been one of the major goals in the study of ultra-low mass objects. However, we have shown in a previous paper (Mohanty et al. 2003a; henceforth Paper I) that the current generation of highly detailed synthetic spectra is equal to the task. Employing these, we have derived gravities to within ± 0.25 dex (and T_{eff} to within ± 50 K) in a sample of very low-mass objects in the Upper Scorpius and Taurus clusters (Paper I). We now derive masses and radii for these, using our Paper I results together with photometry and distance estimates. We will show that our analysis allows mass to be determined to within a factor of ~ 2 , and radius to within $\sim 30\%$. These errors are much larger than those associated, for example, with dynamical mass and radius measurements in eclipsing binaries. Nevertheless, we will demonstrate that they are sufficient for first order tests of the theoretical evolutionary tracks.

Though our analysis is independent of the evolutionary models (and thus serves as a check on the latter), it is clearly dependent on the validity of the synthetic spectra we use. The accuracy of these were discussed in Paper I, and will be addressed further in this work. However, we point out that our derivation of physical parameters using spectral synthesis alone does not constitute a great leap of faith, any more than employing evolutionary models for this purpose does. There are two reasons for this. First, the P - T structure of the deep atmosphere (which forms the inner boundary of the spectral calculations) acts as the outer boundary condition of the interior calculations; i.e., the evolutionary models are anchored with the same (deep) atmospheric modeling as the synthetic spectra. Second, in order to compare observations to the evolutionary predictions, synthetic spectra are crucial: either to convert an observed spectral type to T_{eff} (when placing objects on a theoretical T_{eff} - luminosity H-R diagram), or to convert predicted effective temperatures and luminosities to photometric colors and magnitudes (when placing objects on a theoretical color-magnitude diagram). We have only taken the dependence on synthetic spectra a step further, by using them to derive surface gravities as well; the accuracy of our gravities is discussed at length in Paper I. The advantage of this route lies in our avoiding (and thereby testing) what are perhaps the greatest uncertainties in the theoretical models for young objects: the initial conditions and still-relevant effects of accretion and collapse during the formation stage. The

main disadvantage of eschewing the evolutionary models is that we cannot independently estimate ages. This is compensated for by our ability to independently estimate the mass, and thus provide a check on the evolutionary model predictions for a group of objects that belong to the same cluster, and are thus likely to be (nearly) coeval.

Finally, we elucidate the system of nomenclature we have adopted here for very low-mass objects. There are considerable differences within the community at present regarding this issue: naming conventions based on fusion (or equivalently, mass), origins and location (isolated or in orbit around a star) have all been proposed. Controversies arise because the different definitions do not yield the same grouping of objects; which of these systems is finally adopted is a matter for future arbitration. However, given that a consensus is currently lacking, and that our primary concern in this paper is mass, we adopt a fusion-based convention (since mass is most directly associated with the presence and type of fusion). The term ‘brown dwarf’ refers to all objects which never derive 100% of their luminosity from hydrogen burning (unlike stars), but which are nevertheless above the deuterium-burning mass limit. Thus brown dwarfs are objects in the range $\sim 0.012\text{--}0.080 M_{\odot}$ ($12\text{--}80 M_J$). We contract the term ‘planetary mass object’ to the less cumbersome ‘planemo’, and use it to refer to all objects below the deuterium-burning limit (i.e., mass $\lesssim 12 M_J$), regardless of whether they are free-floating or in orbit around a star. When a distinction is required between the two cases (e.g., when referring specifically to the recent isolated planemo candidates), it will be made explicitly. Since neither planemos nor brown dwarfs undergo stable hydrogen fusion (i.e., reach the Main Sequence), both are included under the rubric of ‘substellar objects’. Since both stars and brown dwarfs undergo at least some fusion, they will collectively be termed ‘fusors’; in this context, planemos are non-fusors. A broader discussion of these terms and nomenclature issues is presented in Basri 2003.

2. Overview of Sample and Observations

A detailed account of our sample selection, observations and data reduction methods, and evidence for cluster membership has been presented in Paper I (also see Jayawardhana, Mohanty & Basri 2002, 2003). We only cite the salient points here. Our sample consists of 11 low-mass Pre-Main Sequence (PMS) objects in Upper Scorpius, ranging in spectral class from M5 to M7.5, and 2 low-mass PMS objects in Taurus - GG Tau Ba (\sim M5.5-6) and Bb (M7.5), which form a close binary within the quadruple system GG Tau. High-resolution optical spectra were obtained for all targets using HIRES on Keck I. The cluster membership and PMS status of the Upper Sco targets were verified using four criteria: presence of Lithium absorption (LiI 6708Å), radial velocity consistent with that of known

Upper Sco members, presence of strong $H\alpha$ emission analogous to that in field dMe stars, and neutral alkali (Na I and K I) line strengths intermediate between those in field dwarfs and giants of similar spectral type. 11 out of an original list of 14 Upper Sco candidates met all four criteria, and are included in our final sample. GG Tau Ba and Bb are previously confirmed PMS members of Taurus; we did not undertake detailed membership tests in their case. The present work also requires photometric and distance measurements. For the Upper Sco targets, we adopt NIR photometry from 2MASS, and optical photometry from Ardila, Martín & Basri (2000; hereafter AMB00, from whose initial photometric survey of Upper Sco our sample is culled). For GG Tau Ba and Bb, we use the optical and NIR photometry cited by White et al. (1999; hereafter WGRS99). Average distances to the Upper Sco and Taurus regions are taken from Preibisch et al. 2002 and WGRS99 respectively.

3. Extinction, Radius and Mass Analysis

Our method of analysis may be summarized thus. We derive extinctions by comparing the observed optical colors ($R_C - I_C$) to those predicted by synthetic spectra for the appropriate T_{eff} and gravity. The radii are then inferred via two slightly different methods. In the first, they are derived by combining the extinctions with the observed I_C -band flux, the predicted I_C -band flux at the stellar surface, and the known distance to the cluster. In the second, the same procedure is followed, but now using J -band fluxes instead of I_C -band ones. Finally, masses are acquired from the radii and the previously derived surface gravities, and luminosities from the radii and previously inferred T_{eff} . Thus, for each object, we have one estimate of extinction from $R_C - I_C$, but two each of radius, mass and luminosity, one from using I_C to determine radius and one from using J . We elaborate on this method in §3.1 below, and quantify our expected stochastic errors in §3.2; the important sources of potential systematic errors are discussed in §3.3. Finally, the rationale for employing $R_C - I_C$ for the extinction calculations, and I_C or J for the radius ones, is also discussed in §3.3.

3.1. Method of Analysis

In Paper I, we derived T_{eff} and $\log g$ for our sample by comparing our high-resolution optical spectra to the latest synthetic spectra by Allard & Hauschildt. The latter have been discussed in detail in Paper I. For our purposes here, it suffices to note that the model spectra have been constructed using plane-parallel atmospheres. As such, they are independent of the stellar radius or mass; they depend only on T_{eff} and gravity, and predict the emergent flux per unit wavelength at the stellar surface. Convolution of the latter with appropriate bandpasses

gives the predicted apparent magnitude *at the stellar surface* in any desired photometric band, for a specified T_{eff} and gravity. This convolution has been carried out for the models, for standard optical and near-infrared passbands¹. For our sample, we also possess observed optical photometry in the Cousins R_C and I_C bands, as well as NIR photometry in the J band. Temperatures, gravities and photometric measurements are listed in Table 1. From these, we calculate extinctions, radii, masses and luminosities as follows.

$$Extinction : \quad A_V = \frac{(R_{Co} - I_{Co}) - (R_{Cm} - I_{Cm})}{k_{RC} - k_{IC}} \quad [1]$$

$$\text{where } k_{RC} \equiv \frac{A_{RC}}{A_V} = 0.81, \quad k_{IC} \equiv \frac{A_{IC}}{A_V} = 0.60 \quad [2]$$

Here, R_{Co} and I_{Co} are the observed magnitudes for a given object. R_{Cm} and I_{Cm} are the synthetic magnitudes at the stellar surface, for the best-fit synthetic spectrum to that object found from our previous T_{eff} and gravity analysis. A_V , A_{RC} and A_{IC} are the extinctions at V , R_C and I_C respectively. The extinction ratios (k_{RC} , k_{IC}) given in equation [2] are taken from Schlegel, Finkbeiner & Davis 1998; they are appropriate for CCD R_C and I_C filters, and a normal extinction law ($R_V \equiv A_V/E(B-V) \approx 3.1$). They imply that $A_V = 4.76E(R_C - I_C)$, in agreement with the relation used by other authors for Upper Sco (e.g., Preibisch et al. 2002). Indeed, $R_V \approx 3.1$ appears to be valid even for the heavily reddened Taurus-Auriga region (9). We therefore assume that a normal extinction law holds for both our Upper Sco sample (following Preibisch et al. 2002), as well as for GG Tau B (in agreement with WGRS99). Note that in the most commonly used procedure for determining extinction, the observed spectrum is first compared to various stellar templates over narrow spectral regions (over which the differential reddening is negligible) to determine the spectral type; the extinction is then derived by comparing the observed colors to unreddened ones at that spectral type. Our method is completely analogous, except that we use synthetic spectra as templates (instead of observed stellar spectra of similar spectral type). Our extinctions are listed in Table 1.

$$Radius : \quad \log_{10} [\mathcal{R}] = \log_{10} [\mathcal{D}] + \left[\frac{I_{Cm} - (I_{Co} - A_{IC})}{5} \right] \quad [3a]$$

or alternatively,

¹Available at <ftp.ens-lyon.fr/pub/users/CRAL/fallard/AMES-Cond-2002/colmag.AMES-Cond.opt6> and [.../colmag.AMES-Cond-2002.ukirt](ftp.ens-lyon.fr/pub/users/CRAL/fallard/AMES-Cond-2002/colmag.AMES-Cond-2002.ukirt)

$$\log_{10} [\mathcal{R}] = \log_{10} [\mathcal{D}] + \left[\frac{J_m - (J_o - A_J)}{5} \right] \quad [3b]$$

Here, \mathcal{R} is the stellar radius and \mathcal{D} the distance to the star (both in parsecs). We adopt $\mathcal{D} = 140\text{pc}$ for GG Tau and 145 pc for our entire Upper Sco sample; these are, respectively, the mean distances to the Taurus star-forming region and to the Upper Sco association. A_{I_C} in eqn. [3a] is calculated from the A_V (eqn. [1]), using eqn. [2]. ($I_{C_o} - A_{I_C}$) is then the I_C magnitude that would be observed on Earth in the absence of extinction; we will often refer to this extinction-corrected value as the ‘intrinsic I_C -band flux’. Similarly, J_m , J_o and A_J in eqn. [3b] are the synthetic J magnitude at the stellar surface, the observed J magnitude, and the extinction in the J -band respectively; A_J is derived from the A_V (eqn. [1]) using $A_J/A_V = 0.28$. ($J_o - A_J$) is then the J magnitude expected on Earth in the absence of extinction; as in the I_C -band case, we will refer to this extinction-corrected value as the ‘intrinsic J -band flux’. The logic behind eqns. [3] is simple: for an unresolved source, in any photometric band, the translation between flux at the stellar surface and the flux finally observed depends upon radius, distance and extinction; any one of these quantities (in our case, radius) can be calculated if all the others are known. We also point out again that, regardless of whether radius is inferred through I_C fluxes or J (eqn. [3a] or [3b]), the extinction used in its derivation is always from $R_C - I_C$ color (i.e., though either A_{I_C} or A_J is used in the radius equations, these are not independently measured quantities but simply calculated from the A_V found through eqn. [1]; thus A_{I_C} and A_J depend only on $R_C - I_C$).

Mass: Mass (\mathcal{M}) is inferred from the radius and previously derived surface gravity, through Newton’s law of gravitation.

Luminosity: Luminosity (\mathcal{L}_{bol}) is inferred from the radius and previously derived T_{eff} .

Clearly, the two radius estimates, one from I_C and the other from J (eqns. [3a] and [3b]), yield two values for mass and luminosity. The rationale for making independent estimates based on I_C and J comes from potential systematics in the synthetic photometry; this is discussed in detail in §3.3 and Appendix A. Both I_C and J -based values are listed in Table 2. In reality, it turns out that the two sets of estimates are in close agreement for most objects: using I_C or J makes no significant difference. The only exceptions are our faintest targets, in which uncertainties in the *observed* optical photometry appear responsible for a divergence between I_C and J . This is addressed in §3.3 and Appendix B; as we argue there, the J -based values should be more accurate for these objects. Consequently, J estimates are good for all our targets; we therefore plot only the J -based values in Figs. 1–4.

3.2. Stochastic Errors

For PMS gravities ($\log g \sim 3.0\text{--}4.0$), $R_C - I_C$ color in the models changes by ~ 0.1 mag for a 100K change in T_{eff} , and by $\lesssim 0.1$ mag for a 1 dex change in gravity. Since our internal errors in derived T_{eff} and gravity are $\sim \pm 50\text{K}$ and ± 0.25 dex (Paper I), the corresponding uncertainties in model $R_C - I_C$ color are $\sim \pm 0.05$ mag and ± 0.025 mag, from T_{eff} and $\log g$ uncertainties respectively. Finally, for Upper Sco, the measurement errors in observed $R_C - I_C$ (see AMB00) are at most of order ± 0.12 mag. Adding all these in quadrature gives a total error of $\sim \pm 0.13$ mag; we adopt ± 0.14 mag (equivalent to adopting 0.1 mag errors both in observed color, and in intrinsic model color due to combined T_{eff} and gravity uncertainties). This leads to an error of ± 0.7 mag in A_V (see eqns. [1] and [2]), which translates to an uncertainty of ± 0.42 mag in A_{I_C} and ± 0.20 mag in A_J .

We also have errors of $\sim \pm 0.15$ mag in the model I_C , due to combined T_{eff} and gravity uncertainties; we adopt 0.2 mag. The errors in observed I_C in Upper Sco (AMB00) are $\lesssim \pm 0.1$ mag; we adopt 0.1 mag. Finally, combining Hipparcos data with an analysis of secular parallaxes constrains the variation about the mean distance to Upper Sco to $\lesssim 20\text{pc}$, assuming a spherical geometry for the association (Preibisch et al. 2002); this translates to $\lesssim \pm 0.06$ dex in $\log_{10}[\mathcal{D}]$. Collecting all these in quadrature, and including the factor of 5 in the denominator of eqn. [3a], gives a final error of ± 0.11 dex in $\log_{10}[\mathcal{R}]$, i.e., $\pm 30\%$ uncertainty in I_C -based USco radii. When J fluxes are employed instead, the internal errors are smaller: while errors in synthetic photometry due to our T_{eff} and $\log g$ uncertainties are similar in J and I_C , extinction errors contribute less in J than in I_C , and the errors in observed photometry are also lower in J ($\lesssim \pm 0.03$ mag from 2MASS). Consequently, our internal errors in $\log_{10}[\mathcal{R}]$ are then ± 0.08 dex, i.e., $\pm 20\%$ uncertainty in J -based USco radii.

Mass is proportional to gravity, and to radius squared. Our uncertainty in $\log g$ is ± 0.25 dex. Combining this with our error in radius gives a final error in $\log_{10}[\mathcal{M}]$ of ± 0.33 or ± 0.30 dex, depending on whether radius is calculated from I_C or J . Our USco masses are thus precise to within a factor of ~ 2 (2.1 for I_C , 2.0 for J). Finally, our ± 50 K T_{eff} error contributes negligibly to the luminosity uncertainty; the latter depends entirely on the error in radius. Our errors in $\log_{10}[\mathcal{L}_{\text{bol}}]$ are therefore $\sim \pm 0.22$ and ± 0.16 dex, for radius based on I_C and J respectively; i.e., our \mathcal{L}_{bol} are uncertain by $\sim 55\%$ (65% for I_C , 45% for J). Finally, for all quantities, our errors for GG Tau Ba and Bb are very similar to those for USco: the uncertainties in their observed photometry, from WGRS99, are comparable to those in USco, and all other errors in our analysis are the same for both clusters.

As noted above, our J -based values have slightly smaller internal errors than the I_C ones. However, to err on the side of caution, we henceforth adopt the higher, I_C -based errors for the J estimates as well. Moreover, for both I_C and J , the fact that our mass and luminosity

estimates are dependent on our radius measurements has an important consequence for the plots shown in §4. When plotting mass or luminosity against radius (or against each other), the X- and Y-axis errors are not independent in our analysis, but coupled. Consequently, the (1σ) errors are illustrated with ellipses, rather than perpendicular error bars.

Finally, we point out that even with a T_{eff} uncertainty of 100K (twice our error in Paper I), we would still obtain radii to within $\sim 35\%$, masses to within a factor of ~ 2.3 , and luminosities to within $\sim 70\%$. These precisions are not much worse than obtained above with a T_{eff} uncertainty of 50K (using the same ± 0.25 dex error in gravity in both cases). Our results are thus quite robust even with T_{eff} errors comparable to those in analyses of low-resolution spectra (e.g., Leggett et al. 2000). Our constraints on mass and radius, substantially better than previously reported from spectral analysis, arise mainly from our well-constrained gravity (± 0.25 dex). As demonstrated in Paper I, the synthetic spectra we use allow this level of precision in $\log g$, even if T_{eff} were uncertain by 100K instead of 50K.

Our foregoing analysis is concerned with internal stochastic errors, i.e., the *precision* of our measurements. This does not address however, the absolute accuracy, or *veracity*, of our values. To assess the latter, we now briefly discuss possible systematic offsets in our analysis. In fact, as we will show, it is the potential for such offsets in the synthetic spectra that dictates the specific color and photometric bands we have chosen to derive A_V and radii.

3.3. Systematic Errors

Our sources of systematic error fall into three categories: (1) offsets in the synthetic photometry, (2) systematic errors in the observed photometry, (3) systematic errors in our adopted T_{eff} and gravity, and (4) real physical phenomena, most pertinently cool spots and binarity. We summarize here the effects of each; details are presented in the Appendices.

Synthetic Photometry: All the parameters in this paper are calculated by comparing the observed photometry and colors of our PMS M-type sample to those predicted by the synthetic spectra. We test the validity of the latter models by comparing them to field M dwarfs. Our conclusion is that, due to possible offsets in the model photometry, extinction (A_V) is best calculated by using $R_C - I_C$ colors (eqn.[1]), while radius (and hence mass and luminosity) is most accurately derived from J -band fluxes (eqn.[3b], where the A_J is directly computed from the A_V implied by eqn.[1]). At the very least, the two radius estimates, from I_C and J respectively (eqns. [3a and b]), should bracket the true value very well. In reality, we find that the radii, masses and luminosities derived from both I_C and J agree very well in the majority of cases (Table 2; $\lesssim 15\%$ difference in \mathcal{R} , $\Rightarrow \lesssim 30\%$ disparity in \mathcal{M} and

\mathcal{L}_{bol}). The only exceptions are objects in which the observed optical photometry appears to be incorrect, as we discuss next; in these, the J -based parameters are more accurate. In conclusion, systematic offsets in synthetic photometry have very little effect on our radii, masses and luminosities. The full analysis is presented in *Appendix A*.

Observed Photometry: In our five faintest objects (USco 100, 109, 112, 128 and 130), the J -based radii are ~ 20 – 40% larger than the I_C ones. We find that this is due to anomalies in their observed fluxes and colors. Comparisons using 2MASS H and K photometry, which are only marginally affected by extinction effects in these objects, reveals that our J -band calculations are likely to be quite accurate, while AMB00’s reported R_C and I_C fluxes (which we use) appear to be uncertain for these five targets (as is quite plausible given their faintness in the optical, close to AMB00’s completeness limits). We therefore adopt the J -based radii, masses and luminosities for these objects. A detailed analysis can be found in *Appendix B*.

T_{eff} and Gravity: Systematic errors in our derived T_{eff} , from spectral analysis, will result in attendant offsets in the synthetic photometry we adopt for any given object, and thus potentially skew our radius calculation. However, we show that such a T_{eff} offset, at the 100–200K level, will in reality hardly affect our derived radii, masses and luminosities: it changes both the derived A_V as well as the adopted surface flux in a given filter, but in opposite senses, so that the net effect is minimal (eg, only a $\lesssim 10\%$ change in radius for a 200K shift in T_{eff}). Gravity offsets, meanwhile, have a negligible effect on the photometry, so do not affect our radii. Errors in $\log g$ will certainly influence our calculated mass directly; however, we present arguments (as we have in Paper I as well) that significant systematics in our adopted gravities (i.e., larger than our adopted ± 0.25 dex measurement uncertainty) are very unlikely. A comprehensive analysis of these issues is presented in *Appendix C*.

Cool Spots and Binarity: We show that even large cool spots (50% areal coverage, 500K cooler than surrounding photosphere) affect our extinction, mass and radius calculations negligibly, while they make us underestimate luminosity by $\sim 25\%$ (mainly due to the 200K lower T_{eff} we infer in the presence of such spots; see Paper I). Large *ultra*-cool spots, covering a significant fraction of the stellar surface and appearing completely dark in a given photometric band compared to the photosphere, can influence our results: with a 50% coverage by a such a spot, we will underestimate radius by a factor of $\sqrt{2}$, and mass and luminosity by a factor of 2 each. Such spots are implausible in any significant fraction of our sample; nevertheless, we do examine if they can be responsible for the very lowest masses we derive (§4.1.1). Binarity, meanwhile, has an effect analogous to cool spots. For equal mass binaries, we will *overestimate* radius by $\sqrt{2}$, and mass and luminosity by a factor of 2. This effect may be responsible for the very highest masses we derive, which appear a little too high for the corresponding spectral types (§4.2). However, since we do not see any double-lined

spectroscopic binaries in our sample, only very close companions (i.e., single-line systems) can skew our results; binarity should not be a large effect for our sample. A full analysis of cool spots and binarity is presented in *Appendices D* and *E* respectively.

4. Results

With these introductory remarks, we move on to a detailed analysis of our mass, radius, T_{eff} and luminosity results. In the course of this, we will repeatedly compare our derived quantities to the predictions of the theoretical evolutionary tracks of the Lyon group. Specifically, in order to encompass a large range in mass, we have combined the tracks presented in Baraffe et al. 1998 (hereafter, BCAH98) and Chabrier et al. 2000 (hereafter, CBAH00), as detailed in Paper I; following the convention in Paper I, we refer to this merged set of tracks as the Lyon98/00 models. These tracks are the ones most widely used in the literature to infer the properties of young, very low-mass stellar and substellar bodies; it is therefore particularly useful to check their predictions against our independently derived values.

Our extinctions, radii, masses and luminosities are listed in Tables 1 and 2. Besides our Upper Sco targets, we have also derived parameters for the well-studied GG Tau B system (Ba and Bb), previously analysed in some detail by WGRS99. For GG Tau Ba, our extinction, mass and luminosity estimates are very similar to those of WGRS99. For Bb, however, our A_V and luminosity are significantly higher, while our mass is $\sim 40\%$ lower (due to the low gravity we find in Paper I). Moreover, our extinction for GG Tau Bb is quite different from that for Ba, at odds with the similar A_V derived for both by WGRS99 (though their A_V for Ba and Bb are not the same as their values for Aa and Ab, the other two components of the GG Tau system). A full discussion of GG Tau, supporting evidence for our extinctions, and detailed comparison to the WGRS99 results is presented in Appendix F. In the following sections, we concentrate on the parameters derived in this paper.

Finally, with regard to radius, mass and luminosity, our discussion will largely be limited to the J -based values: as noted earlier (§3.3), I_C and J yield similar values anyway for most of our objects (Table 2), while in the handful of exceptions (our faintest targets), the estimates derived from J are likely to be more accurate.

4.1. Mass and Radius

In Fig. 1, we plot our derived radii versus mass. Also shown are the Lyon98/00 tracks for various ages, from 1 to 10 Myr. Three striking facts are immediately evident.

First, two of our Upper Sco targets appear to lie close to the planemo boundary of $12 M_J$: J fluxes imply a mass of about $9 M_J$ for USco 128 and $14 M_J$ for USco 130. Our masses are uncertain within a factor of 2, so they may well be brown dwarfs; even so, their position near the bottom of the brown dwarf mass sequence seems secure. These two are our lowest gravity Upper Sco targets, as well as the faintest (Table 1); their ultra-low masses result from a combination of these two factors (e.g., GG Tau Bb, which has a very similar gravity and T_{eff} but is much brighter, has a significantly higher mass of $\sim 25\text{--}30 M_J$). We discuss USco 128 and 130 in more detail in §4.1.1.

Second, for masses $\gtrsim 0.03 M_\odot$, our mass-radius relationship agrees remarkably well with that predicted by the Lyon98/00 tracks at the expected ages of Taurus (1–1.5 Myr) and Upper Sco (3–5 Myr). However, third, there is a significant discrepancy between our radii and the predicted ones for the lowest masses ($\lesssim 0.03 M_\odot$), with our values being considerably higher. GG Tau Bb has a radius twice that expected for a 1–1.5 Myr old, $30 M_J$ object. Similarly, for their masses, USco 128, 130 and 104 all have radii almost twice that predicted for an age of 3–5 Myr, and $\sim 40\text{--}50\%$ larger than expected even at 1 Myr. For USco 104, the offset might conceivably arise from our analysis uncertainties: its position is consistent with the 3–5 Myr tracks within our errors in mass and radius. For GG Tau Bb and USco 128 and 130, though, our result is robust in spite of the estimated errors. This result can also be stated in terms of age: given our radii, the Lyon98/00 models suggest that our lowest mass objects are much younger than higher mass ones in the same clusters.

Note that objects that agree/disagree with the track predictions in the mass-radius plane are the same ones that are most consistent/inconsistent with the tracks in our T_{eff} -gravity plot in Paper I (see Fig. 9 in Paper I). This is not coincidental, since our masses depend on gravity; we address this shortly in our analysis of the radius discrepancy (§4.1.2).

It is noteworthy here that, regardless of our deviation from the Lyon98/00 tracks at the lowest masses, our derived masses and radii agree with two broad theoretical predictions, which are largely independent of the particular evolutionary models used. One is that PMS objects of any given mass contract with age. The other is that within a coeval sample, lower masses should generally have smaller radii (with some scatter introduced by any age spread, as well as by the details of the contraction process). Our results clearly exhibit both trends: the Taurus objects GG Tau Ba and Bb, which should be younger than the Upper Sco sample, are indeed somewhat larger than similar mass bodies in Upper Sco, while our inferred radii within both clusters also distinctly decrease with decreasing mass. This result is heartening, given the spread in T_{eff} , gravities and A_V in our sample, and the possible errors in the calculation of each; it bolsters our confidence in the derived parameters.

We now analyze in some detail the two major results of our mass/radius calculations:

the surprisingly low masses derived for USco 128 and 130, and the radius discrepancy with the tracks at the low-mass end of our sample. In §4.1.1, we delve into the underlying reasons for the apparent near-planemo status of the two Upper Sco objects, and show that our result is reasonably robust in the face of various possible sources of error. In §4.1.2, we examine whether systematic errors discussed earlier (§3.3) can explain our larger-than-predicted radii for the lowest masses, and conclude that they cannot; real problems seem to exist in the theoretical evolutionary models at these masses. We then show, in §4.2, that the evolutionary tracks may be problematic even at the higher masses, where our results are so far in apparent agreement with the tracks. Finally, we discuss our conclusions in §5.

4.1.1. Planemos

We find a mass of 9 M_J for USco 128 and 14 M_J for USco 130, using J fluxes (I_C fluxes predict even lower masses, of 6 and 7 M_J respectively (Table 2); since the latter are likely to be spurious for these two faint targets (§3.3), we focus on the higher, more accurate J values). At the estimated age of Upper Sco (3–5 Myr), the theoretical evolutionary tracks predict that masses $\lesssim 15 M_J$ have $T_{eff} \lesssim 2300\text{K}$; planemos (mass $\lesssim 12M_J$) have $T_{eff} \lesssim 2100\text{K}$; and masses $\lesssim 10M_J$ have $T_{eff} \lesssim 2000\text{K}$. Our derived temperature for both objects, though, is about 2600K (comparable to our values for other mid- to late M’s in the sample). Our mass estimates thus present a rather severe temperature discrepancy (300–600K) with the theoretical expectations. Moreover, we find USco 128 and 130 to have the same T_{eff} , but much lower mass, compared to GG Tau Bb (whose T_{eff} is more consistent with the tracks for its mass); this is at odds with the steep decline in T_{eff} with decreasing mass predicted by the Lyon models (§4.2). Our masses for USco 128 and 130 thus deserve greater scrutiny.

USco 128 and 130 have the lowest gravities in our Upper Sco sample, with $\log g \approx 3.25$ dex. However, this is not the main reason behind their very low inferred masses. This is best illustrated by comparing them to GG Tau Bb. All three have similar spectral types ($\sim M7-7.5$), and our T_{eff} from spectral analysis are correspondingly nearly identical. Moreover, their gravities are all about the same; if anything, our gravity for GG Tau Bb ($\log g \approx 3.125$) is slightly *lower* than in the other two (Table 1). Despite these close similarities, our mass for GG Tau Bb is $\sim 30 M_J$: a value which is not particularly remarkable, and more importantly, is 2–3 times larger than our estimates for USco 130 and 128 respectively. Low gravity alone, therefore, does not account for the ultra-low masses we find in the latter two targets. Instead, the primary reason is their considerable faintness compared to GG Tau Bb. After correcting for extinction, we find USco 130 to be 1 mag fainter than Bb in J , while USco 128 is 1.5 mag fainter. Since our distance and T_{eff} for all three are nearly identical,

we are led to ascribe this faintness to a reduction in surface area; consequently, our radii for USco 130 and 128 are much smaller (by a factor of 1.6 and 2 respectively) than for GG Tau Bb. Since our gravities for the three are nearly the same, our masses derived using $\mathcal{M} \propto g \mathcal{R}^2$ are correspondingly far lower in the USco objects than in Bb. Specifically, compared to Bb, \mathcal{R}^2 in USco 130 and 128 is lower by a factor of 2.5–4, while their gravities are only a factor of 1.3 (0.125 dex) higher; hence they come out to be 2–3 times less massive than Bb.

Of course, even if USco 128 and 130 were the same mass as GG Tau Bb, we would expect their radii to be smaller through contraction, since they are older. However, the evolutionary models predict that this is not a very large effect, in the mass range of interest here. Specifically, WGRS99 have found GG Tau Bb to have $T_{eff} \sim 2800\text{K}$ and mass $\sim 40 M_J$, by assuming that the theoretical evolutionary tracks are accurate. Without making any such assumption, we have derived $T_{eff} \sim 2600\text{K}$ and mass $\sim 30 M_J$. It appears safe to assume, therefore, that GG Tau Bb lies somewhere in this range (though we prefer our values). From Fig. 1, we see that objects in this mass and T_{eff} interval are expected to shrink in radius by at most $\sim 25\%$ (0.1 dex), in going from an age of ~ 1 to 5 Myr. The same conclusion can be drawn from Fig. 9 in Paper I, which shows that the predicted gravity increases from 1–5 Myr by at most 0.25 dex, and usually by much less, for these masses/temperatures. Our derived $\log g$ difference of 0.125 dex between GG Tau Bb and the two USco objects is thus fully consistent with this expectation (though our *absolute* values of $\log g$ for these three objects diverge substantially from the model predictions, which is one of the main results of Paper I); as we have seen, planemo masses are derived in spite of this (small) increase in gravity. Even the maximum, $\sim 25\%$ contraction predicted by the model tracks is insufficient to explain the factor of 1.6–2 decrease in radius in going from GG Tau Bb to USco 130 and 128, implied by their observed difference in brightness.

It may be suggested that the difference in brightness between GG Tau Bb on the one hand, and USco 128 and 130 on the other, is not intrinsic, but is an artifact of inaccuracies in our derived A_V : the extinctions we use for correcting the observed J fluxes in USco 128 and 130 are derived from AMB00, and we have shown in Appendix B that these A_V values are probably somewhat incorrect, due to errors in AMB00’s R_C and I_C photometry in the faintest objects. However, we have also argued in Appendix B that any resulting A_V offsets are unlikely to significantly alter the intrinsic J fluxes we have derived. In particular, we have shown that comparisons using H and K photometry, which are even less affected by extinction than J , strongly support the claim that USco 130 and 128 are indeed intrinsically 1 and 1.5 mag fainter than GG Tau Bb respectively. The A_V we have derived modify the observed J , H and K magnitudes only marginally; even if we assume $A_V=0$ for all three objects (since our extinctions may be overestimated; Appendix A), USco 130 remains 1 mag fainter than GG Tau Bb in the NIR, while USco 128 is still ~ 1.3 mag fainter (implying a

mass of $11 M_J$, quite similar to the $9 M_J$ derived using our A_V (Appendix B). Realistic differences in A_V cannot account for this; USco 128 and 130 do appear intrinsically faint.

Similarly, it is unlikely that large ultra-cool spots make the two USco objects anomalously faint: such spots would have to cover 60–75% of the surface, and remain dark compared to the photosphere all the way out to K . Such extremely large and cool spots are unlikely in any one object in our relatively small sample, let alone in two: indeed, the cool spot in this case would constitute the real photosphere, with the ‘true’ photosphere reduced to a ‘hot spot’. Distance uncertainties alone also seem incapable of producing the underluminosity of USco 128 and 130 compared to Bb. Distances to both Upper Sco (145 pc) and Taurus (140 pc) are uncertain by ~ 20 pc; USco 130 and 128 thus remain underluminous by a factor of 1.3–2 even if we simultaneously assume that GG Tau is closer by 20 pc, and USco 128 and 130 farther by the same amount. Finally, one may invoke the exotic scenario of close-to edge-on disks around USco 128 and 130. Such orientations however, are very rare, and it is unlikely that two of our targets are affected by them. Moreover, neither of these objects shows strong signatures of ongoing accretion (JMB02), and there is no evidence for any excess $K-L'$ disk emission at least around USco 130 (USco 128 shows a moderate $K-L'$ excess; Jayawardhana et al. 2003). Together, these facts make it rather improbable that nearly edge-on disks cause the underluminosity of both USco 128 and 130.

It is true that a combination of offsets in gravity, distance and photometry can lead to USco 128 and 130 having significantly higher masses, more consistent with that of GG Tau Bb, even if individually these factors are insufficient for this purpose. This is illustrated in Fig. 1, where our upper limits in mass for the two USco objects are seen to be compatible (or nearly so) with Bb. However, factors of 2–3 underestimations in mass are not apparent in any of our other targets; if anything, a few of them appear somewhat too massive (perhaps due to binarity). Thus, while we cannot completely rule out USco 128 and 130 having masses close to that of GG Tau Bb, we believe that our much lower estimates, close to the planemo boundary, are fairly robust. Our conclusion certainly needs to be thoroughly checked through further observations; the (distant) possibility of edge-on disks should also be pursued.

4.1.2. Analysis of Radius Discrepancy

The second important result from our mass-radius analysis is that our coolest, lowest mass objects seem to have larger radii than predicted for their masses, at the expected cluster ages. In §3.3.3, we have outlined various systematics that may influence our results. We now examine whether any of these can lead to the radius discrepancy, and find that they cannot.

Notice first that, apart from uncertainties in gravity (which we return to shortly), all the other systematics - errors in synthetic and observed photometry, T_{eff} offsets, binarity and cool spots - affect mass only through their influence on radius (since we use Newton’s law to derive mass from radius and gravity). That is, at a given gravity (inferred from spectral analysis), all these systematics cause our targets to move along locii on which $\mathcal{M} \propto \mathcal{R}^2$.

Next, notice that at a given age, the evolutionary models predict approximately the same gravity for masses ranging from planemos to well into the stellar domain (Fig. 9, Paper I). The only deviations from this are in the stellar/brown dwarf regime at the earliest ages (1–2 Myr), where assumptions about initial conditions related to deuterium-burning produce some larger variations in gravity (Paper I), and in very low-mass planemos, where the early onset of degeneracy makes $\log g$ decrease with mass (due to nearly constant radius). To restate: while the gravity of a given mass increases with age as it contracts, gravity is predicted to generally remain nearly constant with mass (or equivalently, T_{eff}) at a given age (for the range of masses, T_{eff} and ages of interest here). The mass-radius tracks simply reflect this near constancy in gravity: i.e., a track at a specified age closely traces a locus of $\mathcal{M} \propto \mathcal{R}^2$, where the constant of proportionality is the gravity predicted for that age (this is why the tracks are nearly straight lines in the logarithmic mass-radius plot shown in Fig. 1, except at the youngest ages and at low planemo masses).

Taken together, these considerations have two implications. First, the aforementioned systematics, which directly influence radius, only cause our targets to slide *parallel* to the theoretical tracks in the mass-radius plane. Thus, invoking these systematics cannot improve (or detract from) the agreement between the tracks and our results. Notice that the stochastic errors considered in §3.2 (again barring gravity; see further below) are also largely incapable of changing whether or not we lie on a specific mass-radius track, for the same reason: they directly affect only radius, thus moving objects parallel to the track locii.

Second, the compatibility of our results with the theoretical mass-radius tracks depends primarily on how well our gravities agree with the predicted values. Say our inferred $\log g$ for an object matches the (nearly constant) value predicted by the evolutionary models for its age. Then, since our mass depends on our measured gravity through Newton’s law, we are bound to fall *somewhere* along the mass-radius track for that age, regardless of the precise radius we derive. Altering the radius will certainly change the inferred mass, but the object will still remain on the same track, which corresponds to a particular gravity. Conversely, if our $\log g$ diverges from the model value for some age, we will also be offset from the corresponding mass-radius track at that age, no matter what radius we infer.

The above analysis reveals why all the targets whose $\log g$ were found to be consistent with the Lyon98/00 predictions for their assumed ages, in Paper I, also line up on the

appropriate mass-radius locii in Fig. 1. It is also clear why GG Tau Bb, USco 128 and USco 130 lie so far from the theoretical mass-radius locii: their inferred gravities are much lower than the model predictions for their expected ages (Paper I). The crucial point is that uncertainties in radius (either systematic or stochastic) cannot alter these results².

Errors in gravity, on the other hand, which affect mass directly while influencing radius negligibly, can potentially be invoked to explain the radius discrepancy between our results and the Lyon tracks for the coolest, lowest mass targets. Specifically, consistent underestimations in gravity for low T_{eff} objects will shift them horizontally to spuriously low masses in Fig. 1, making their measured radii appear too large for their mass. However, we have already argued exhaustively, both here (Appendix C) and in Paper I, against significant systematics in our $\log g$; we do not consider this a likely explanation. With respect to stochastic errors, it may be suggested that the radius discrepancies are evident only when we employ 1σ (0.25 dex) uncertainties in $\log g$; if, by fluke, our adopted gravities are in error by more than this, GG Tau Bb and USco 128 and 130 may be consistent with the tracks. However, as noted above, what is really needed is a systematic underestimation of gravity. It is very unlikely that this could arise by chance from random measurement errors, in all three of our coolest objects (all four, if one counts the less significant, but similarly directed deviation of USco 104 from the tracks). Evidence that our stochastic errors in $\log g$ are small also comes from the absence of horizontal deviations from the evolutionary models at higher masses. Since gravity hardly affects our radii, measurement uncertainties in $\log g$ will manifest themselves as large offsets in mass alone; no such appear at masses $\gtrsim 0.03 M_{\odot}$ (i.e., at higher masses, our gravities are remarkably consistent with the model predictions for the estimated ages; this is also apparent in the $T_{eff} / \log g$ plot in Fig.9 of Paper I). Deviations only at the lowest masses, and all in the same direction, argue strongly against large stochastic errors in $\log g$.

In conclusion, neither systematic nor stochastic errors in our analysis seem adequate to explain the disagreement in radius between the evolutionary model predictions and our values for the coolest, lowest-mass objects. This prompts us to suggest that the evolutionary models may themselves be problematic. We reached the same conclusion from our $T_{eff} / \text{gravity}$ analysis in Paper I (not surprising, since our compatibility with the mass-radius tracks

²This analysis is certainly valid for the Upper Sco sample (estimated age 3–5 Myr): by $\gtrsim 3$ Myr, the Lyon $\log g$ at a given age are indeed nearly constant with mass and T_{eff} . It is also valid for GG Tau Bb, even though the Lyon $\log g$ are *not* constant at ~ 1 Myr: our gravity for Bb is less than the *lower limit* of Lyon values for this age (for any plausible mass or T_{eff} ; Paper I), so Bb must be offset from the Lyon 1 Myr mass-radius track regardless of the radius we derive. GG Tau Ba is more complicated, and addressed in §4.2. We can ignore it for now, since it does not appear discrepant on the mass-radius plot.

depends on our agreement with the model gravities). In both cases, using our parameters in conjunction with the theoretical tracks implies that the cooler (lower-mass) objects are much younger than the hotter (higher-mass) ones. In Paper I, we argued that this age mismatch is spurious, both for our Upper Sco sample and (especially) for the two components of GG Tau B. We further argued that the mismatch is caused by theoretical model uncertainties for the coolest objects, which is what we are also suggesting here as well. The possible nature of these uncertainties was discussed in detail in Paper I; we touch on them again in §5.

4.2. Radius and Mass versus T_{eff}

It might appear from the above discussion that at least the higher-mass objects ($>30M_J$), which agree with the Lyon98/00 models in both the temperature-gravity and mass-radius planes for their expected ages, are not a source of concern. However, an inkling that all might not be well even in this mass regime comes from a consideration of GG Tau Ba.

Compare the position of this object in the T_{eff} -gravity plot (Fig. 9, Paper I) to its position in the mass-radius one (Fig. 1). At the T_{eff} we infer, GG Tau Ba lies quite far in gravity from the 1 Myr Lyon98/00 track in the T_{eff} - $\log g$ plane; at the same time, it agrees very well with the 1 Myr mass-radius track. This can only happen if our temperature for Ba is at odds with the evolutionary models: specifically, the gravity we derive is consistent with the Lyon98/00 1 Myr track only at a $T_{eff} \sim 200\text{K}$ higher than our inferred value (Fig. 9, Paper I). This effect is obvious for GG Tau Ba only because the theoretical tracks evince comparatively large variations in gravity with changing T_{eff} at the youngest ages (due to initial condition effects, as discussed earlier). In the Upper Sco targets, any such temperature offsets are largely masked in the T_{eff} -gravity plane by the near constancy of $\log g$ at a specified age: objects can slide horizontally along the T_{eff} axis while continuing to agree with the predicted gravity. As we have shown in the last section, such agreement with the Lyon models in $\log g$ alone will also produce agreement with these models in the mass-radius plane, again without hinting at the underlying inconsistency in T_{eff} . In short, conflicts in temperature at Upper Sco ages cannot be probed via a simple comparison between the temperature-gravity and mass-radius planes, as is possible at the age of GG Tau. We must explicitly compare mass and radius individually to T_{eff} , as we now proceed to do.

In Fig. 2 and Fig. 3, we plot our radii and masses against T_{eff} , and compare to the Lyon98/00 tracks. In both cases, substantial discrepancies are apparent between our results and the theoretical models for the higher mass objects ($> 30M_J$). For the temperatures we derive, their masses and radii appear significantly larger than the tracks suggest; equivalently, the models are hotter by $\gtrsim 200\text{K}$ than our values, for their inferred mass or radius. Now, our

four highest derived masses ($\sim 0.20\text{--}0.25 M_{\odot}$; see Table 2) do seem slightly too high, given their spectral types (all our objects are M5 and later); in the field, $0.25 M_{\odot}$ corresponds roughly to M4, while M5 and later correspond approximately to masses $\lesssim 0.15 M_{\odot}$ (e.g., see Delfosse et al. 2000). Unrecognized binarity is an effect that will preferentially move objects to both larger radii and higher masses in our technique (Appendix E). If our highest mass objects were nearly equal-mass binaries, they would actually be $\sim 0.12 M_{\odot}$, i.e., closer to the track predictions for their T_{eff} . Since the translation between spectral type and T_{eff} or mass has not really been tested for young low-mass objects, the viability of this possibility is a priori unclear; binarity should be checked through follow-up observations.

It is hardly likely, however, that every one of our higher-mass objects is a binary. Even if this were true, the T_{eff} discrepancy with the tracks would remain (though reduced to $\sim 100\text{K}$). Moreover, numerous studies show no evidence of binarity in GG Tau Ba (and our mass of $0.12 M_{\odot}$ is consistent with that of field objects of the same spectral type, $\sim\text{M6}$). The fact that our T_{eff} for this object also diverges from the Lyon models by $\sim 200\text{K}$ suggests that binarity is not the key problem here. All this points to a real disagreement in temperatures.

The Lyon98/00 evolutionary models use, as an outer boundary condition, significantly older versions of the Allard & Hauschildt synthetic spectra, while we use an updated one. It is known that the older generations of these spectra yield higher T_{eff} for field M dwarfs than the newer ones do (e.g., compare the results of Leggett et al. 1996 to Leggett et al. 2000). Moreover, the new spectra provide much better fits to the observed M dwarf spectral energy distributions (SEDs); the newer dwarf T_{eff} thus appear more trustworthy (Leggett et al. 2000). Extending this to our PMS sample, the T_{eff} we derive for our objects using the new synthetic spectra are also likely to be more accurate than any values derived using older versions. This may explain the difference between our T_{eff} and those in the Lyon98/00 models: the suggestion is that the Lyon models find hotter temperatures than our (presumably more accurate) values because they use older synthetic spectra.

Although attractive, this suggestion is not necessarily correct. The reason is that, while the evolutionary models indeed use the atmospheric calculations as an outer boundary condition, the actual T_{eff} (and luminosity) implied by the models for a given mass is primarily a function of the interior calculations, and only slightly dependent on the atmospheric properties: the atmosphere in these objects is a very thin skin that is rather inconsequential for the evolutionary modeling. For instance, much of the improvement in the newer synthetic spectra results from the use of updated opacities. However, the temperature and luminosity evolution of these low-mass bodies is only marginally allied to photospheric opacity: $L(t) \propto \kappa_R \sim^{1/3}$, $T_{eff}(t) \propto \kappa_R \sim^{1/10}$ (Burrows & Liebert 1993). Whether this slight dependence, combined with the difference in opacities between the older and newer spectra, is sufficient

to give the $\sim 200\text{K}$ change in T_{eff} we require, is doubtful. Similarly, the newer synthetic spectra incorporate a more likely convective mixing-length parameter (α) of 2 (as discussed in Paper I, $\alpha \approx 2$ in both the upper and deep atmospheres is suggested by the latest 3-D hydrodynamic models for both PMS and field M dwarfs, while the older spectra and the Lyon98/00 tracks use $\alpha=1$). However, BCAH02 show that this change in α appears important only for about the first million years, and hardly affects the Lyon models at later ages (for the masses of concern here), while our USco objects are supposed to be at $\sim 5 \pm 2$ Myr.

Thus, while the new synthetic spectra are crucial for our T_{eff} determination from spectral analysis, and are hence instrumental in revealing uncertainties in the theoretical evolutionary tracks (assuming the spectral new spectral models are accurate), it is not clear that simply incorporating these new atmospheric calculations in the evolutionary modeling is by itself sufficient to remove the discrepancy between our results and the track predictions. It is possible that the problem lies deeper, in the interior calculations of the evolutionary models.

On the other hand, it is useful to examine the alternative hypothesis, that the Lyon98/00 temperatures are in fact correct, and it is our spectroscopically derived T_{eff} that are amiss. In Paper I, we have shown that the synthetic spectra employed reproduce the spectral features of our PMS sample remarkably well. They also match the observed SEDs of field dwarfs much better than previous versions, as mentioned above. However, these results do not, by themselves, rule out systematic offsets in the implied temperatures (e.g., due to inaccuracies in model opacities). Is it possible that such systematics in our T_{eff} are responsible for our conflict with the Lyon models? We think not, for the following reason. Our T_{eff} are determined through a fine-analysis of the TiO bandheads, which are only marginally dependent on gravity. Gravities, meanwhile, are deduced from the profiles of the absorption doublets of Na I and K I. However, the latter lines depend sensitively on both temperature and gravity. To fix $\log g$ uniquely, therefore, the temperature is fixed at the value implied by the TiO bandheads. Consequently, if the model treatment of TiO is inadequate, leading to systematic offsets in the derived T_{eff} , then we will derive the correct $\log g$ only if the synthetic spectra err in their treatment of the alkali lines as well - and fortuitously by just the right amount, in both Na I and K I, to offset the independent error in T_{eff} from TiO. Given the completely independent parameters that enter into determining the behaviour of each of these species - TiO, Na I and K I - this would be quite a remarkable coincidence, and is not tenable. It is far more likely that if our T_{eff} are wrong, then our gravities are wrong as well. However, we have seen that our gravities actually agree with the Lyon98/00 values for the higher-mass objects, for their estimated ages. If our $\log g$ are incorrect in this mass and age regime, then it would appear so are the Lyon ones. While such simultaneous offsets in both our and the Lyon values are possible, they are untestable without additional empirical constraints. Moreover, this hypothesis simply replaces our original suggestion of a T_{eff} error in the Lyon models with

an error in Lyon gravities. It is more reasonable to suppose that, when our independently derived $\log g$ match the Lyon predictions, both values are correct. If so, it is hard to see how our spectroscopic T_{eff} for the higher masses could be far off the mark. It is worth noting in this regard that problems in the theoretical mass- T_{eff} relationship are also emerging in stars that are somewhat higher in mass ($\sim 0.6\text{--}1 M_{\odot}$) than those considered here, through studies of field and PMS eclipsing binaries (Torres & Ribas 2002; Stassun et al. 2003). Various shortcomings in the evolutionary models, such as in the treatment of convection, have been proffered to resolve this issue (Stassun et al. 2003; Montalbán et al. 2003). It remains to be seen if similar effects are also applicable in the mass regime of interest here, and whether they can bring the Lyon temperatures into better agreement with our values.

Finally, we point out that our temperatures for the lowest-mass objects (GG Tau Bb, USco 104, 128 and 130) are either consistent with, or *higher* than, the Lyon values in the mass- T_{eff} plot, in contrast with the situation at the higher masses (Fig. 3). In the radius- T_{eff} plane, on the other hand, they appear cooler than the Lyon predictions for their radii, just like the more massive objects (Fig. 2). This apparent contradiction in the behaviour of the low-mass bodies, when compared to the Lyon tracks - seemingly too cool in one parameter space, and too hot in another - clearly cannot be due solely to a temperature offset from the tracks. Instead, its genesis lies in the fact, discussed earlier, that our gravities for these objects are incompatible with the Lyon values at any plausible T_{eff} . Specifically, their offset from the tracks in the radius- T_{eff} plane can be attributed to their radii being too large for their inferred temperatures (just like their radii are larger than predicted for their mass). Notice the subtle difference in interpretation of the radius- T_{eff} plot for the higher and lower masses: in the former, the divergence from the Lyon tracks arises from a disagreement in T_{eff} , while in the latter it arises primarily from a discordance in radius, even though the final result looks the same (all the objects appear younger than expected in the radius- T_{eff} plane). Meanwhile, the mass- T_{eff} plot points to an *additional* offset in temperature at the two lowest masses (USco 128 and 130), which appear hotter than predicted for their inferred mass³.

³Fig. 3 shows that uncertainties in our mass for these two objects can potentially reduce this T_{eff} discrepancy, by bringing them closer to the position of GG Tau Bb. However, we have already presented in §4.1.1 arguments in support of our derived mass, and are fairly confident that mass errors are not the problem here. Notice, furthermore, that increasing their mass estimate, to agree more closely with that of GG Tau Bb, requires us to either increase the gravity at fixed radius, or increase the radius at fixed gravity. This cannot alter, and can instead exacerbate, the offset of these objects from the Lyon radius- T_{eff} tracks (just as GG Tau Bb is offset from the latter tracks, even though it agrees with the mass- T_{eff} ones).

4.3. Mass versus Luminosity

Finally, our mass-radius and mass- T_{eff} results can be combined to examine the mass-luminosity relation in our sample (Fig. 4). We saw that in masses $\gtrsim 0.03M_{\odot}$, our radii agree with the Lyon98/00 predictions for the expected ages (~ 3 -5 Myr for Upper Sco and ~ 1 Myr for Taurus), while our T_{eff} are lower than predicted for the same ages and masses. At lower masses, our radii are much larger than predicted, while our T_{eff} are roughly consistent with, or larger than, the predicted values. Since $\mathcal{L}_{bol} \propto \mathcal{R}^2 T_{eff}^4$, these results lead us to find luminosities that are slightly lower than indicated by the models for masses $\gtrsim 0.03M_{\odot}$ (for the expected ages), and substantially greater than predicted for lower masses.

Notice that the luminosities for the higher masses are actually quite close to the theoretical ones, especially given our error bars (though they are slightly systematically lower than expected for the ages indicated by the mass-radius plot). This is because our T_{eff} disagreement with the models for these masses ($\gtrsim 200K$), though large in absolute terms, constitutes a relatively small fractional discrepancy ($\sim 7\%$). This, combined with the good agreement with the models in radius, yields luminosities that are roughly in agreement with the theoretical ones. At lower masses, however, our radii are a factor of ~ 2 larger than in the models, resulting in a substantial divergence between our luminosities and the theoretical ones (this is compounded at the lowest masses - USco 128 and 130 - by our inferred T_{eff} also being much larger than the predicted ones).

Notice also that, in the Lyon evolutionary tracks, lower (higher) luminosity at a given mass corresponds to an older (younger) object. This is because evolution in these models proceeds roughly along vertical Hayashi tracks over the first few Myr: a given mass contracts with age (modulo deuterium-burning, which slows the contraction rate) at approximately constant T_{eff} (see Fig. 2). Our results show the same luminosity trend: both components of GG Tau, which are expected to be younger than the Upper Sco objects, are more luminous than the latter. This is a direct consequence of the fact that we find the GG Tau components to have a larger radius than similar mass but older Upper Sco targets (Fig. 1).

5. Conclusions

Young star-forming regions contain a set of objects at similar distance, with similar ages and compositions. They are usually extensively studied photometrically, yielding colors. Combining photometry with spectra (which yield temperatures), one can determine extinctions and luminosities. These can then be leveraged to determine radii. Finally, high-resolution spectra can provide surface gravities, and thereby masses when combined with the

radii. These stellar parameters, obtained with the aid of model atmospheres, can then be compared with those from theoretical isochrones, allowing a calibration of the fundamental evolutionary calculations that have been heavily used in the analysis of star-forming regions.

In a previous paper, we used “fine analysis” of high resolution-spectra of young, very low-mass objects to gain reasonably precise temperatures and gravities. In this paper, we use the photometry of these objects as described above to complete a measurement of their fundamental stellar parameters. Taking observational and model atmosphere errors and uncertainties into account, we reach two major conclusions:

(1) Both radius and T_{eff} decrease less rapidly with diminishing mass, at a given young age, than predicted by the theoretical evolutionary models. Specifically, in the mass-radius plane the lowest mass objects ($\lesssim 30 M_J$) remain much larger (i.e., contract more slowly with age) than the models suggest, while the higher masses have radii in good agreement with the model predictions. In the mass- T_{eff} plane, the higher masses are substantially cooler than predicted, while the lowest masses have T_{eff} either in better agreement with, or hotter than, the model values. The combination of these two trends implies that luminosity also falls off less dramatically with mass, at a given age, than the evolutionary models indicate.

(2) The lowest masses in our Upper Sco sample are near the deuterium fusion boundary.

Because of the importance of both conclusions, we have taken considerable pains to consider possible sources of error, both observational and systematic. These include conversion of colors to extinctions, temperature scales for pre-main sequence objects, problems with the gravity measurements, and the effects of starspots or binarity. Our extinctions are consistent with an analysis of the same region using low dispersion spectra. Our temperature scale is in good agreement with recent photometric work in the field. The range of masses we find within a few spectral subclasses is perhaps surprising, but we show that some of our basic conclusions can be drawn just from the observations (without recourse to theory at all). We conduct a comparative analysis with a more extensively-studied young (GG Tau B) binary system to further test our conclusions, and find comparable discrepancies with theory in that case as well. Finally, our derived relationships between radius, mass, T_{eff} and luminosity all agree (within the measurement uncertainties) with certain basic theoretical predictions that are likely to be correct regardless of evolutionary model uncertainties: younger objects have larger radii than older ones of the same mass; less massive objects are cooler and generally smaller than more massive ones at a given age; and luminosity decreases with both diminishing mass (at fixed age) and increasing age (at fixed mass). There does not appear to be any a priori physical basis, therefore, for discarding our results. We also point out that (like the Lyon models) our mass-radius, mass- T_{eff} , radius- T_{eff} and mass-luminosity relationships are smooth, without any sharp breaks or discontinuities. The precipitous drop in gravity at low

temperatures that we found in Paper I, which might seem remarkable at first sight, is due (if our analysis is correct) simply to a relatively slow change in radius and T_{eff} (compared to the Lyon predictions) over a significant range in mass.

The weight of the evidence suggests that substantially more work should go into the measurement of physical parameters of young substellar objects, the validity of the evolutionary tracks, and, without doubt, further testing and confirmation of our results. An especially important conclusion of our work is that agreement with the evolutionary models in any single two-parameter plane (e.g., mass-radius) does not guarantee agreement in all parameters (e.g., T_{eff} , luminosity). In order to ascertain the veracity of the models, their predictions must be checked for all the parameters, not just a selected few. As a corollary, comparing an object to the evolutionary models over one set of parameters (e.g., T_{eff} -luminosity), in order to estimate other quantities (e.g., mass), is an exercise that is not always justified. Such translations, which are common practice in current studies of young low-mass objects, may lead to spurious mass and radius estimates, and must be undertaken with great caution. Similar conclusions have been reached by other authors, in the context of evolutionary model comparisons to higher-mass (solar-type) PMS stars (e.g., Torres & Ribas 2002).

In Paper I, we pointed out some specific areas of concern for theory, such as accretion effects and the treatment of convection and deuterium fusion. In particular, we noted that if deuterium fusion begin at an earlier time than predicted, the discrepancies in radius and gravity between the theoretical tracks and our measurements, for the lowest masses, may be resolved. This is a testable hypothesis, as we outlined in Paper I, and bears closer examination. In this paper, we have also identified discrepancies in the theoretical T_{eff} predictions (assuming our derived temperatures are accurate), especially for the higher mass objects in our sample. The underlying physical basis for temperature uncertainties in the evolutionary models is unclear; it is possible that remaining inadequacies in the treatment of convection are at fault. Finally, while the model atmospheres and synthetic spectra that lie at the heart of our analysis are tremendously improved from earlier generations, they still suffer from certain shortcomings. Specifically, they reproduce the photometry of field M dwarfs in some, but not all, of the optical and infrared bands. While we have gone to great lengths to account for, and exclude, any attendant uncertainties in our analysis, further improvements in the atmospheric modeling - particularly in the linelists and opacities (most importantly, of H_2O) - would be tremendously useful for future studies of field and PMS low-mass objects.

We have implemented methods that have long been used for normal stars. They provide a means of testing theoretical isochrones and obtaining fundamental stellar parameters for very young, very low-mass objects. This methodology (which highlights the importance of high resolution spectroscopy and model atmospheres) should also be extended to higher mass

objects and other star-forming regions with different ages. Extensive programs of this nature are now both desirable and feasible.

We would like to acknowledge the great cultural significance of Mauna Kea for native Hawaiians, and express our gratitude for permission to observe from atop this mountain. We would also like to express our thanks to the Keck Observatory staff, who have made possible, and successful, our observations over the last several years. We would like to thank Russel White for kindly supplying two of the spectra used in this paper. We would also like to thank Russel White, Lee Hartmann, Gilles Chabrier and Isabelle Baraffe for illuminating discussions on PMS evolution, and a constant readiness to help. S.M. would like to acknowledge the support of the SIM-YSO grant for his postdoctoral research. This work was supported in part by NSF grants AST-0205130 to R.J. and AST-0098468 to G.B.

A. Model Colors and Photometry

To date, there are no empirical measurements of intrinsic colors and surface fluxes in cool, low-mass PMS objects, precluding any direct tests of the synthetic photometry in this regime. However, Leggett et al. 2000 have recently derived temperatures for a number of similarly cool (but older) field M dwarfs with known distances. We evaluate the reliability of the model photometry through comparisons with these objects, and assume, with appropriate caveats, that similar results hold in the cool M-type PMS regime.

We have specifically analysed field dwarfs with solar metallicity, and $T_{eff} \approx 2600\text{--}3000\text{K}$ (corresponding to M5–M6.5 types in Leggett et al’s study), since abundances in our PMS objects are likely to be solar (Paper I), and their T_{eff} from spectral analysis lie in the same range. Moreover, we have focussed on behaviour in the R_C , I_C and J bands: the field and PMS objects are intrinsically too red for accurate shorter wavelength photometry, while the synthetic spectra are known to have some problems related to H_2O opacity in the H and K bands (Leggett et al. 2000), the investigation of which is beyond the scope of this paper.

Within these constraints, Fig. 5 shows that the synthetic spectra reproduce the field dwarf $R_C\text{--}I_C$ colors remarkably well: theory and observations agree to within $\pm 0.1\text{--}0.2$ mag, with no evident systematic offsets. $R_C - J$ and $I_C - J$ are worse, with the synthetic colors being clearly bluer by $\gtrsim 0.2$ mag (extinction should be negligible for these nearby Main Sequence stars). Thus, assuming a similar situation holds in the PMS regime, $R_C - I_C$ appears best suited to derive A_V for our targets; hence our use of this color index (eqn. [1]).

On the other hand, Fig. 5 reveals that the *absolute* photometry of the field dwarfs is best reproduced by the synthetic spectra in the J band. The models are too bright in R_C and I_C by upto ~ 0.5 mag, but only by < 0.2 mag in J . Indeed, this appears to explain the color behavior noted above: the overluminosity of the models in R_C and I_C compared to the observations, combined with the more accurate J -band predictions, makes the synthetic $R_C - J$ and $I_C - J$ colors too blue; simultaneously, the errors in model R_C and I_C fluxes, similar in magnitude and direction, cancel to make the $R_C - I_C$ predictions commensurate with the data. At any rate, the synthetic J -band fluxes seem most appropriate for estimating the true surface flux, and hence radius, in M-type field dwarfs, and by extension in our M-type PMS sample. Using model I_C (or R_C) to calibrate the true surface flux (once extinction is corrected for using $R_C - I_C$) will, if the field dwarf results apply to the PMS regime, cause us to underestimate radius, and hence mass and luminosity (basically, we will assume that the stellar surface is brighter per unit area than it really is, in R_C or I_C , thus requiring a spuriously low surface area, or radius, to produce a given A_V -corrected observed flux). In fact, the synthetic I_C fluxes do appear overluminous compared to J in the PMS regime: our I_C -radii are systematically somewhat lower (on average by $\sim 20\%$) than the J ones (§4).

However, there is also some evidence that the synthetic $R_C - I_C$ colors, while accurate for the field dwarfs, suffer from systematic offsets for our PMS sample. On the one hand, our inferred Upper Sco extinctions are commensurate with those found by Preibisch et al. 2002 for their Upper Sco PMS targets of similar spectral type (A_V derived using a method complementary to ours). However, the Upper Sco region is known to have very little remaining nebulosity, and $100\mu\text{m}$ surveys towards the region indicate an average $A_V \sim 0.5$ mag, about 1 mag less than our mean value. Nebulosity on small spatial scales, surrounding the individual stars, might account for this discrepancy. Alternatively, it is possible that the PMS model $R_C - I_C$ are systematically too blue by ~ 0.2 mag, leading us to overestimate A_V by ~ 1 mag (i.e., A_{I_C} and A_J by ~ 0.6 and 0.3 mag respectively).

Such an offset in extinction would have the following consequence. If our synthetic J -band surface flux estimates are accurate (as the field dwarf results suggest), then overestimating A_J by 0.3 mag would produce corresponding overestimations in radius, mass and luminosity (15%, 30% and 30% respectively). Conversely, if our model I_C surface fluxes are too high (again as indicated by the field dwarfs), combining them with the erroneous extinctions would actually yield reasonably *correct* radii, masses and luminosities: the proposed systematic error in A_{I_C} (~ 0.6 mag) is about equal to that in I_C flux (~ 0.5 mag in the field), but the two offsets act in opposite directions - higher A_{I_C} implies larger radius, while higher I_C flux at the stellar surface implies lower radius - and thus largely cancel out (eqn. [3]).

To summarize: field dwarf comparisons indicate that the synthetic $R_C - I_C$ colors and J -band surface fluxes are accurate, while the model I_C surface fluxes are too high. Assuming this holds for our PMS sample, our extinctions and J -based radii, masses and luminosities are accurate, while the I_C -based values are underestimations. However, our extinctions may be too high due to model $R_C - I_C$ offsets in the PMS regime. In this case, the values inferred using I_C fluxes continue to be lower than those from J , but the I_C -based parameters are in fact more accurate, while the J ones are overestimations. We cannot currently distinguish between the two possibilities. However, the I_C and J calculations should reasonably bracket the true values. We thus provide both sets of estimates (Table 2); our primary conclusions (§4) remain unaltered independent of which set is adopted. In fact, in the majority of cases our parameters from I_C and J are very similar (Table 2): radii agree to within $\sim 15\%$, and thus masses and luminosities to within $\sim 30\%$. In the few cases where this is not true, errors in the observed optical photometry are likely to blame, as addressed in Appendix B.

Finally, the possible overluminosity in the synthetic I_C fluxes may raise some questions about the validity of our T_{eff} and $\log g$ inferred from spectral analysis (Paper I), since most of our spectral diagnostics lie in the I_C band. This issue is addressed in Appendix C.

It is worth pointing out here the pitfalls associated with analysing PMS low-mass objects

based on spectral type considerations alone, as is common practice in current research. Any such analysis requires assumptions about intrinsic PMS colors and photometry, in order to derive extinctions, luminosities and so on. As Fig. 5 shows, colors are strongly dependent on T_{eff} and (to a lesser extent) gravity. Thus, using spectral types to derive PMS parameters requires an accurate translation from spectral type to T_{eff} and $\log g$. Such a translation, however, is at present sorely underdeveloped. Most investigators assume field M dwarf colors for low-mass PMS objects; however, the spectral-type to T_{eff} conversion for field dwarfs remains uncertain by roughly $\pm 100\text{K}$ (e.g., Leggett et al. 2000). Moreover, PMS gravities are considerably lower (by 1–2 orders of magnitude) than those of field objects. Both effects can lead to significant errors in assigning PMS colors (see Fig. 5). More importantly, it is not at all clear that PMS temperatures are the same as that of field dwarfs, for a given spectral type. Indeed, the most widely adopted PMS T_{eff} scale these days is that of Luhman 1999, who advocates PMS T_{eff} systematically higher, by $\sim 100\text{--}200\text{K}$, than in field dwarfs of the same spectral type. This PMS T_{eff} scale is based on the *requirement* that PMS observations agree with the Lyon98/00 theoretical evolutionary tracks, and is thus completely model-dependent. Nevertheless, assuming it is qualitatively correct (i.e., that PMS T_{eff} are higher than dwarf ones), it is obvious that field dwarf colors are not appropriate for the PMS domain. In particular, many analyses of M-type PMS objects simultaneously assume (1) intrinsic colors similar to that of field dwarfs (for calculating extinctions and luminosities), and (2) the Luhman 1999 T_{eff} scale (for putting the PMS objects on an H-R diagram). The concurrent adoption of both assumptions is internally inconsistent, and untenable.

The attraction of using spectral types for PMS analysis, clearly, lies in the ease with which types can be determined. Nevertheless, spectral types are a purely empirical construct. In order to employ them profitably, it is imperative to derive a priori the connection between types and physical conditions. In particular, the above discussion shows that one must first establish (without recourse to evolutionary model predictions) a spectral type to T_{eff} conversion scale for the PMS regime. Detailed spectral analyses, such as undertaken in Paper I, are necessary to accomplish this. Of course, our present work (Paper I and here) includes only a small sample, and covers a very limited range in spectral types. It is thus insufficient to derive a robust spectral type - T_{eff} scale for PMS objects (nor is the derivation of such a scale our intent in this work). Future studies with larger samples must address this issue. The crucial point, however, is that our analysis eschews spectral type considerations; we explicitly derive T_{eff} and $\log g$ for our PMS targets, and then use the appropriate colors and photometry (based on model atmosphere calculations). In so doing, we avoid the current uncertainties associated with spectral type to temperature, gravity and color conversions.

B. Errors in Observed Photometry

In three of our targets (USco 100, 109, 128), the J -band radii are more than 20% higher than the I_C -band ones; in two others (USco 112 and 130), they are more than 30% higher. This is surprising, given that in all the remaining objects the discrepancy is $\lesssim 15\%$, and mostly less than 10% (Table 2). It cannot be due to synthetic photometry problems that increase with changing T_{eff} or gravity: the temperatures and gravities of the five anomalous objects span the range derived for our entire sample, and other targets at these T_{eff} and $\log g$ present no difficulties. A closer look reveals that these five are also our faintest targets (Table 1). This leads us to propose that the disagreement between their I_C and J values is due to systematically larger errors in their observed optical photometry (i.e., in R_C and/or I_C , adopted from AMB00) than in the other, brighter objects. This suggestion is driven by the appearance of color anomalies in these faintest targets, as we now show.

For the sake of concreteness, we compare USco 130 (which exhibits the largest radius anomaly: a 40% difference between I_C and J) and GG Tau Bb (whose I_C and J radii are nearly identical). From spectral analysis (independent of reddening), we have found nearly identical T_{eff} for the two; regardless of any systematics in our precise T_{eff} value, the equivalence of their temperatures is robust, given the close similarity between their TiO bands (which are highly sensitive to T_{eff} differences and negligibly to gravity; Paper I). Thus, since photometric colors depend predominantly on T_{eff} and very marginally on gravity (which we find to be nearly the same in both anyway), we expect their intrinsic colors to be very similar. However, this expectation is not borne out. After accounting for extinction, USco 130 is fainter than GG Tau Bb by ~ 2 mag in R_C and I_C , but by only ~ 1 mag in J . In other words, its A_V -corrected $R_C - I_C$ color is the same as Bb's (which is guaranteed since we derive A_V from $R_C - I_C$), but its $I_C - J$ and $R_C - J$ are much redder. Analogous discrepancies occur regardless of which pair of bands A_V is calculated from. The problem can be traced directly to the observed photometry (Table 1). We see that USco 130 and Bb have exactly the same observed $R_C - I_C$ (2.46 mag), but USco 130 appears far redder in $I_C - J$ (3.16 vs. 2.39 mag) and $R_C - J$ (5.62 vs. 4.85 mag).

This behavior is very difficult to recreate through physical effects. Given two stars with the same T_{eff} , extinction differences cannot redden $I_C - J$ and $R_C - J$ and leave $R_C - I_C$ unchanged. Ultra-cool spots, by contributing increasing flux with longer wavelength, can potentially be responsible. In reality, however, the R_C , I_C and J bands are too close together for this to produce any large effect: spots too cool to contribute much flux in R_C and I_C compared to the photosphere (thus leaving $R_C - I_C$ unchanged) also do not yield significant flux relative to the photosphere in J (and so do not change $I_C - J$ or $R_C - J$ much either). The same is true for cooler companions, whose effect is akin to that of spots (Appendix D).

Another alternative is the presence of excess NIR flux from a disk. However, such emission should be minimal in J . Moreover, there is no evidence for any substantial circumstellar material around USco 130: neither any high-resolution spectral signatures of disk-accretion (JMB02), nor any excess emission even at longer NIR wavelengths ($K-L'$), where it should be far more evident than at J (Jayawardhana et al. 2003). Finally, our J -band photometry for the USco sample is from 2MASS; the errors in this are $\lesssim 0.03$ mag, much too small to produce the above effects. It is thus safe to conclude that a spuriously high J flux, engendered either by real phenomena or errors in observed J , cannot account for USco 130 being redder in $I_C - J$ and $R_C - J$ than GG Tau Bb. At the same time, uncertainties arising from synthetic photometry errors cannot be responsible. Since the observed $R_C - I_C$ is the same in both, and so is their T_{eff} , their implied A_V must also be very similar, independent of the precise extinction we derive using model colors. If the A_V is the same in both, then the other observed colors ($I_C - J$, $R_C - J$) should also be the same, for photospheres at the same T_{eff} . The only remaining solution is that the observed R_C and/or I_C photometry for USco 130 is incorrect. This can lead to the sort of effects we see, as illustrated shortly.

A comparison of the H and K photometry for USco 130 (from 2MASS) and GG Tau Bb (from WGRS99) supports the above hypothesis. The observed values are $H = 13.54$, $K_s = 13.08$ for USco 130, and $H = 12.38$, $K = 12.01$ for Bb (the intrinsic offset between the K_s and K filters is negligible for our purposes and can be ignored; Carpenter 2001). We see that in both filters, USco 130 is fainter than GG Tau Bb by ~ 1.1 mag, a similar reduction in flux as in the observed J band (Table 1). Correcting H and K by our derived extinctions does not change this result: USco 130 remains ~ 1 mag fainter than Bb in both bands, just like in A_V -corrected J . The fact that accounting for extinction does not affect the flux difference between USco 130 and Bb is of course not surprising, given that our A_V for both is nearly the same. However, the point is that the difference between the two objects in H and K agrees with that in J , and not with the ~ 2 mag difference in R_C and I_C . Since all the arguments above supporting the accuracy of the J photometry are equally applicable to H and K , we are once again led to conclude that the observed R_C and I_C values are incorrect.

Note that, since USco 130 is fainter than Bb by similar amounts in all three NIR bands, their observed NIR colors are very alike. As we find their T_{eff} to be the same, this might suggest that their extinctions are also identical, just as implied by the equivalence of their $R_C - I_C$ colors. In that case, the R_C and I_C fluxes quoted by AMB00 would both have to be underestimations by nearly 1 mag, in order to obtain the same flux difference in the optical as in the NIR without altering the derived A_V . This is implausible. However, J , H and K are actually very insensitive to extinction, compared to R_C and I_C . Thus for any reasonable variation in A_V between USco 130 and GG Tau Bb (see below), the observed differences in their NIR colors will still closely reflect their intrinsic differences. Thus, what

their resemblance in NIR colors really implies is that their T_{eff} are indeed very similar, as we claim. Small variations in A_V and reasonable errors in R_C and I_C are still perfectly admissible, as we now show.

With the available information, it is impossible to uniquely determine the errors in observed R_C and I_C . However, we can still run a plausibility check by considering likely values. Imagine that the R_C magnitude quoted by AMB00 for USco 130 is too high (i.e., R_C flux too low) by 0.3 mag, and the I_C too high by 0.4 mag. If so, USco 130 is also 0.1 mag redder in $R_C - I_C$ than the AMB00 value; our extinction estimate must therefore increase by 0.47 mag (bringing the total A_V difference between USco 130 and Bb to $0.47+0.14 = 0.61$ mag; see Table 1). Correcting for these offsets produces a difference of 1.1 mag between USco 130 and GG Tau Bb, in both R_C and I_C . At the same time, the change in A_V alters our previous estimates of intrinsic J , H and K by $\lesssim 0.1$ mag; USco 130 then remains ~ 1 mag fainter than Bb in the NIR. Thus, the optical and NIR differences between the two are now completely consistent. Notice that AMB00’s quoted errors in R_C and I_C are $\lesssim 0.1$ mag. However, they cite no increase in errors with decreasing brightness, which seems rather unrealistic given that their sample covers ~ 5 magnitudes in R_C and I_C , with the faintest objects (including the anomalous ones discussed here) lying near or below their completeness limit in R_C and I_C (~ 19 and 18.5 respectively). We think it quite within the bounds of reason, therefore, to postulate 0.3–0.4 mag errors in R_C and I_C for USco 130, which is the faintest target in our sample (and among the very faintest in AMB00’s). Of course, the above exercise is not proof that these are indeed the precise errors in R_C and I_C . It serves to demonstrate, however, that (1) plausible uncertainties in the observed optical photometry can easily explain the discrepancy between the optical and NIR bands in USco 130, and (2) the J photometry is likely to be more accurate (i.e., not subject to significant change upon correcting for these uncertainties), and thus the J -based radius more trustworthy (notice that, once the optical photometry is corrected in the illustrative exercise above, the I_C radius, as expected, becomes consistent with the J one, just as it is in GG Tau Bb).

Similar arguments can be made for USco 128. From 2MASS, we have $H = 13.78$ and $K_s = 13.21$ for this object. Its observed difference with Bb ($H=12.38$, $K=12.12.01$; WGRS99) is then 1.40 and 1.20 mag in H and K respectively, very similar to the 1.25 mag difference in observed J (Table 1). Accounting for our derived extinctions yields intrinsic H and K differences of 1.53 and 1.28 mag; once again, consistent with the 1.5 mag intrinsic difference we derive in J . For USco 130, we have illustrated that correcting for discrepancies between its (erroneous) optical and (more accurate) NIR photometry probably leads to a change of $\lesssim 0.1$ mag in the intrinsic J , H and K derived using A_V based on AMB00 photometry. In USco 128, the divergence between the optical and NIR photometry is even smaller than in

130⁴, so the intrinsic J , H and K we derive for it, and the corresponding offsets from GG Tau Bb in these filters, should be quite accurate. In other words, H and K photometry, which is even less affected by A_V errors than J , supports the claim that USco 128 is 1.5 mag fainter than GG Tau Bb; if we conservatively adopt the observed photometry without any A_V correction, the difference between the two in the NIR is still ~ 1.3 mag (implying $11 M_J$ for USco 128, close to our adopted estimate of $9 M_J$ and still in the planemo regime).

Analogous conclusions can also be drawn for the three remaining anomalous objects, by comparing them to targets at similar T_{eff} and gravity that do not exhibit large differences between I_C and J radii (e.g., compare the discrepant object USco 112 to USco 75). Specifically, their observed R_C and I_C fluxes from AMB00 appear too low. It is this underluminosity (combined with attendant offsets in A_V), which we claim is spurious just as in USco 130, that ultimately results in their I_C radii (and hence masses and luminosities) being significantly lower than the J ones. Note that, since the divergence between I_C and J radii is smaller in these targets than in USco 130, the required corrections to their observed R_C and I_C are also correspondingly lower. At any rate, the implication, as in USco 130, is that the parameters derived from their J photometry are more dependable than the I_C -based ones. In all the other targets, using I_C or J makes little difference.

C. T_{eff} and Gravity

It may be that our T_{eff} and $\log g$, inferred from detailed comparisons to synthetic spectra, are systematically erroneous (due to systematics in the model spectra). In Paper I we argued that these errors should be quite small. Nevertheless, it is fruitful to examine the consequences of such offsets for our present calculations. In the last section, we found evidence for some systematics in the synthetic photometry, at least in the field M dwarf regime. In the present analysis we assume that, notwithstanding any such absolute offsets, at least the differential model photometry is correct: i.e., that the models accurately predict the *change* in colors and fluxes for a given shift in T_{eff} or gravity. Under this assumption, we first investigate the effect of systematic T_{eff} and $\log g$ offsets on our derived extinctions, radii and so on. We then discuss the feasibility of such systematic errors in temperature and gravity, in light of the synthetic photometry results discussed in the last section.

⁴The apparent difference between USco 130 and GG Tau Bb in the optical, after A_V correction, is 2 mag, while in the NIR it is 1 mag; this is the discrepancy we ascribe to errors in AMB00’s photometry for USco 130 (§3.3.2). In USco 128, the corresponding values are 2 mag and 1.5 mag, so the optical and NIR values are divergent by only 0.5 mag, implying a smaller correction to the AMB00 photometry for the latter object.

In §4.2, we show that our T_{eff} are generally lower than the evolutionary track predictions, by up to 100–200K. *If* this is due to an underestimation in our T_{eff} (and we argue in §4.2 that it is not), then our adopted synthetic photometry must be altered as well, to reflect the new temperatures; we wish to calculate the resulting change in our other parameters. Now, every 100K rise in T_{eff} (in the T_{eff} range of interest here, 2500–3000K) produces a decrease in model $R_C - I_C$ by ~ 0.1 mag, and a decrease in model I_C and J magnitudes by ~ 0.2 and 0.15 mag respectively; i.e., the star is predicted to become both bluer in $R_C - I_C$, and brighter in I_C and J . For a given observed $R_C - I_C$, the change in model color implies A_V larger by ~ 0.5 mag, i.e., an increase in A_{I_C} and A_J by 0.3 and 0.15 mag respectively. However, as discussed in §3.3.1, simultaneous increases in both extinction and estimated surface flux act in opposite senses in the radius calculation (eqns. [3a,b]): the net change in inferred radius is then very small. For a 100–200K rise in T_{eff} , the numbers above imply an increase in radius by only 5–10% when I_C fluxes are employed, and a corresponding increase in mass and \mathcal{L}_{bol} by just 10–20%; with J fluxes, the changes are even less. These offsets are clearly insignificant compared to our adopted stochastic errors of 30%, factor of 2, and 65% in radius, mass and luminosity. We are thus confident that our values for the latter parameters are largely unaffected by the photometric effects of any plausible systematic offset in T_{eff} . Notice, however, that since we calculate luminosity through $\mathcal{L}_{bol} \propto R^2 T_{eff}^4$, a 100–200K rise in T_{eff} will directly raise our \mathcal{L}_{bol} estimates by a further ~ 15 –30% (in addition to the modification discussed above, which arises due to the photometry-related change in radius).

Similarly, we have found large (0.50–0.75 dex) variations in gravity within our sample, at odds with the evolutionary track predictions (Paper I). If our $\log g$ are in error, then the attendant offsets in adopted synthetic photometry might lead to errors in our other parameters as well. However, it turns out that changes in gravity produce very small offsets in the synthetic photometry. For instance, even a 1 dex offset in our $\log g$ alters the model $R_C - I_C$, I_C and J by <0.1 , $\lesssim 0.1$ and <0.05 mag respectively. Our radii, and hence masses and luminosities, are thus negligibly affected by gravity-induced photometric errors.

However, gravity offsets will certainly affect mass directly and strongly, through our use of Newton’s law to derive mass, independent of gravity-related photometric effects (which affect mass via tiny changes in radius). In Paper I, we have already argued extensively against large systematic uncertainties (greater than our measurement errors of ± 0.25 dex) in our inferred $\log g$, based on both a detailed evaluation of the synthetic spectra as well as purely empirical inter-comparisons of the observed spectra. In particular, our tests there strongly suggest that the large gravity variations in our sample are due neither to physical effects such as dust, cool spots and metallicity fluctuations, nor to problems in the synthetic spectra arising, for example, from an inadequate treatment of collisional broadening. However, we showed in §3.3.1 that the synthetic I_C fluxes appear systematically higher than observed in

field M dwarfs; by extension, such an effect may also occur in our PMS sample. Since most of our spectral diagnostics in Paper I lie within the I_C -band, it is instructive to dwell for a moment on the implications of any such overluminosity for our T_{eff} and gravity results.

For a given T_{eff} , the surface flux per unit area, σT_{eff}^4 , is fixed; too much flux in any spectral region must then be compensated for by too little in others. An overluminosity in I_C then implies that either (1) the model continuum opacity in I_C is too low, allowing too much flux to escape in this bandpass (and correspondingly too little in others), or (2) the opacity in some other bandpass(es) is artificially high (leading to the same effect). It is the first possibility that is a cause for concern, since synthetic opacity problems in I_C can cause errors in our T_{eff} and $\log g$, derived from modeling of spectral lines within this bandpass. Specifically, TiO bandheads form our main temperature diagnostic; this molecule is also the main continuum opacity source in the optical for M-type objects. If the synthetic spectra underestimate the TiO opacities, then our T_{eff} estimates will be too low (because the model bandheads at a given T_{eff} are too weak, forcing us to choose cooler temperatures to match the data). Concurrently, our gravities will also be spuriously low: at the low T_{eff} inferred from the TiO bandheads, the Na I doublet (our main gravity diagnostic) will be too strong (since Na I strength depends on both T_{eff} and gravity; Paper I), and we will adopt an artificially low gravity in order to match the observed doublet profile (assuming the model treatment of Na I itself, which contributes negligibly to the continuum opacity, is correct).

The above is a qualitative argument. It is by no means certain, though, that erroneous TiO opacities will actually permit simultaneous good fits to both the Na I doublet as well as the surrounding continuum, as we obtain in Paper I. Secondly, fits to K I give us gravities consistent with those from Na I; since K I and Na I differ in their T_{eff} /gravity dependencies, this is unlikely to happen if our temperatures are significantly inaccurate. Thirdly, the M dwarf comparisons show marked I_C overluminosity over our entire PMS T_{eff} range; as such, we should underestimate gravity for all our targets. However, our $\log g$ disagree substantially with the evolutionary tracks only for the cooler objects; the hotter ones agree very well with the tracks. Fourthly, as a corollary, we should not find gravity variations between objects at the same temperature (i.e., with similar TiO bandhead strengths), which is nevertheless seen in our sample (Paper I). These considerations strongly indicate that the overluminosity in synthetic I_C is not due to opacity problems in the I_C -band itself, but in other bandpasses (see below). In this case, our T_{eff} and $\log g$ should be accurate: even if excessive flux is pushed out over the entire I_C -band, our spectral analysis, dependent only on the relative interplay between continuum and various line opacities within I_C , remains unaffected.

In this context, it is noteworthy that significant discrepancies remain in the model treatment of H_2O , which is the main source of continuum opacity in the near-infrared. The

linelists appear incomplete, and disagreements are apparent between the models and observed low-resolution NIR spectra (1; Leggett et al. 2000). Thus, given the above arguments, and the remarkably good and consistent fits we obtain to our I_C -band spectral diagnostics, we think it far more probable that any overluminosity in the I_C bandpass is due to an inadequate treatment of H_2O in the NIR (namely, an overestimation of H_2O opacity, probably in the H and/or K bands), and not problems in I_C opacities. Consequently, we expect our T_{eff} and $\log g$ values to be reasonably accurate, without substantial systematic offsets.

D. Cool Spots

We now consider the possible effects of cool surface spots on our analysis. The main result is that cool spots, covering up to 50% of the stellar surface and cooler than the surrounding photosphere by up to 500K, do not affect our results significantly. Such spots causes us to underestimate T_{eff} from spectral synthesis by at most $\sim 200\text{K}$ (see also Paper I for a more detailed discussion of this); for our targets, with T_{eff} in the range $\sim 3000\text{--}2500\text{K}$, this leads to an ‘underestimation’ of luminosity by $\sim 25\%$ (whether this is a true error is a matter of taste, since such a large cool spot does lower the luminosity below the value expected from an unspotted, hotter photosphere). Moreover, the extinction, radius and mass estimates are affected negligibly. Fundamentally, these quantities depend on the *difference* in T_{eff} derived from the spectral synthesis and from the photometry, while the presence of a spot (cooler than the photosphere by $\lesssim 500\text{K}$) affects both the spectra and the photometry similarly. Finally, spots that are either closer in temperature to the photosphere, or smaller than we assume, affect our results even less.

However, a large *ultra*-cool spot could affect our conclusions. Such a spot would be completely dark against the stellar surface and contribute insignificant flux; thus, its effect on T_{eff} from spectral synthesis, and on extinction, would be negligible. However, if its areal coverage is a good fraction of the stellar surface, the star will be fainter than in the absence of the spot, leading us to underestimate radius and mass. For a dark spot covering 50% of the surface, our inferred radius would be too small by a factor of $\sqrt{2}$, and mass too low by a factor of 2; for a more plausible 30% coverage, the respective underestimations are $\sim 15\%$ and 30%. In §4.1.1, we address this scenario with respect to some of our targets.

We reach the above conclusions by modeling the effect of spots using the synthetic spectra predictions for various photospheric temperatures. We consider only differences in T_{eff} between the cool spot and the surrounding photosphere, and neglect any differences in gravity (see Paper I for a discussion of those). This approach is vindicated by the synthetic spectra, which indicate that changes in T_{eff} affect the photometric fluxes and colors much more than

changes in gravity do; it is also supported by comparisons between giant and dwarf photometry by other authors (e.g., Gullbring et al. 1998). We will concern ourselves here only with R_C , I_C and J band photometry, since these are the bands we use for our extinction, mass and radius analyses. We will also assume that both the observed photometry and the high-resolution spectra are affected by spots with similar T_{eff} and covering fraction, despite the fact the photometry for our targets was obtained a few years before the spectra (this is further discussed at the end of this Appendix). For the sake of argument, we assume the unspotted photosphere to have $T_{eff} = 3000\text{K}$ and $\log g = 4.0$ (as in the spot discussion in Paper I); the results for other T_{eff} and gravities within the range of our interest ($T_{eff} \sim 2500\text{-}3000\text{K}$, $\log g \sim 3.0\text{-}4.0$) are very similar. We first consider spots cooler by 500K than the surrounding photosphere (i.e., spot $T_{eff} = 2500\text{K}$), and covering half the stellar surface; we then discuss the effect of much cooler spots. We also recall here, from the spot discussion in Paper I, that under these assumed conditions (3000K photosphere, 2500K spot, $\log g = 4.0$, covering fraction=50%), our *spectral* analysis of Paper I would imply $T_{eff} \approx 2800\text{K}$. This fact will become useful in the following discussion.

For the T_{eff} assumed for the spot and unspotted photosphere, the peaks of their spectral energy distributions are in the NIR, and the R_C and I_C bands lie in the Wien part of their spectra. Consequently, the cooler spot contributes more flux in I_C than in R_C . This immediately implies that the intrinsic $R_C\text{-}I_C$ color of the spotted star will be that of an object cooler than the photospheric temperature of 3000K (but no cooler than the spot temperature of 2500K). For a rough a priori estimate (checked below through detailed examination of the synthetic spectra), we may assume that the R_C , I_C and J fluxes scale as the bolometric flux. In this case, with the spot covering half the surface, the resulting flux in all three bands (and thus the $R_C\text{-}I_C$ color as well) will be similar to that from an object with $T_{eff} \approx 2800\text{K}$ ($= [(3000^4 + 2500^4)/2]^{1/4}$).

These expectations are confirmed by our analysis of the photometry predicted by the Allard and Hauschildt models. We combine the model fluxes for a 3000K and a 2500K object, both at $\log g = 4.0$. We find that the resulting R_C , I_C and J band fluxes correspond to T_{eff} of ~ 2825 , 2800 and 2775K respectively. The intrinsic $R_C\text{-}I_C$ color of the spotted star is found to correspond to $T_{eff} \sim 2875\text{K}$. Note that these photometric temperature estimates are very similar to the $T_{eff} \approx 2800\text{K}$ that would be derived for the same spotted star from our spectral analysis of Paper I. What does this imply for our extinction, mass and radius analysis? As detailed in §3, we infer A_V by comparing the $R_C - I_C$ color implied by our derived T_{eff} and gravity (from spectral fits), to the observed color. We then derive radius by combining the observed J magnitude, synthetic J magnitude expected at the stellar surface (given our derived T_{eff} and gravity), A_V and distance. Consequently, our derived A_V , radius and mass will be affected by cool spots, only if there is a substantial *difference* between the

T_{eff} inferred from our spectral fits and that suggested by the intrinsic photometry ($R_C - I_C$ color and J magnitude).

The results above show that the T_{eff} difference is negligible, even for a large spot that is cooler than the surrounding photosphere by $\sim 500\text{K}$. The spectral lines and $R_C - I_C$ color are almost identically affected by the spot; the T_{eff} inferred from them differ by only $\sim 75\text{K}$ (which is of order the $\pm 50\text{K}$ uncertainty in our T_{eff} determinations anyway). According to the models, this leads to a difference between intrinsic and assumed $R_C - I_C$ color of only 0.08 mag, and hence an error in A_V of only ~ 0.4 mag. Even without accounting for cool spots, our uncertainties in T_{eff} and gravity determination and in the observed photometry lead to A_V errors of ~ 0.7 mag (§3.3). Moreover, most of our derived A_V are $\gtrsim 1$ mag, much larger than the cool spot effect. For both reasons, cool spots affect our A_V results negligibly.

Now the radius determination involves, apart from A_V (and distance), the observed J -band flux and that expected from our derived T_{eff} . However, we showed above that (modulo distance) the intrinsic J -band flux will be the same as that expected from our spectral fits (i.e., both indicate almost exactly the same T_{eff}) even when cool spots are present, so differences in J -band flux due to cool spots can be neglected as an additional source of error for radius determination. The A_V errors due to cool spots *will* contribute, but marginally so as discussed above, since they are much less than both our A_V uncertainty due to other causes, as well as the absolute A_V values we find without considering cool spots. The same holds true for our mass derivation. Note here that we have also used I_C fluxes, instead of J , to compute an alternate set of radius and mass estimates for our sample (see §3.3 and Appendices A and B). However, the same arguments apply to I_C fluxes as well: the intrinsic I_C flux of the spotted star corresponds to the same T_{eff} as derived from our spectral fits, so the presence of the spot does not affect our I_C -based radii and masses. To summarize, we do not expect even large spots, cooler than the surrounding photosphere by $\sim 500\text{K}$, to affect our A_V , radius and mass derivations to any significant degree. Hotter or smaller spots, of course, will affect us even less, since they will imply a T_{eff} , in both observed photometry and in the spectral lines, that is even closer to that of the unspotted photosphere.

What about much cooler spots? Since they will contribute negligible flux compared to the hot photosphere, they will not affect our T_{eff} , gravity and A_V determinations. However, if they cover a large fraction of the stellar surface, the observed I_C -band flux will be much less than that in the absence of the spot. If the spot covers half the surface, we will underestimate radius by factor of $\sim \sqrt{2}$, and underestimate mass by a factor of 2. However, we consider it unlikely that such an effect is strongly affecting our results, since spots this large are expected to be rather rare. The usual covering fraction is more like 30%, which will cause us to underestimate radius by $\sim 15\%$ and mass by $\sim 30\%$. We discuss the effect of such spots

on our results in the main body of the text (§4.1.1).

Our luminosity estimates may also be affected by the presence of spots, either because we infer a T_{eff} that is less than that of the photosphere (by $\sim 200\text{K}$, as discussed above and in Paper I), or because a large fraction of the star appears dark due to a large ultra-cool spot. However, we emphasize that the luminosity we then infer is not erroneous, but a true indicator of star’s energy output. A star covered by a large cool spot *is* less luminous than it would be without the spot (keeping the T_{eff} of the unspotted photosphere constant).

Finally, we assume that the spot coverage is the same during the photometric and spectroscopic observations, though the two were not obtained simultaneously (separated by $\lesssim 4$ years in all cases). If the spot covering fraction were much larger when the photometry was obtained, then the star will appear redder (i.e., cooler) in the photometric measurements than in the spectroscopic ones. Consequently, we would overestimate extinction, radius, mass and luminosity. The opposite occurs if the spot coverage were significantly lower during the photometric observations. Without knowing a priori the magnitude of temporal variations in spot coverage in our sample, it is impossible to precisely quantify the resultant errors.

However, as discussed above, spots affect our analysis only if they cover a large fraction ($\gtrsim 50\%$) of the surface. If the covering fraction is this large, then its temporal variations might be comparatively small (assuming the spotting is not concentrated in one place). While individual spots may appear and disappear, it is unlikely that a very heavily spotted star will become, over only 4 years, a comparatively unspotted one, or vice versa (stellar cycles are not thought to occur in such young objects). Thus, assuming the spot coverage is relatively unchanged between the photometric and spectroscopic observations seems fairly reasonable. If, on the other hand, the spot covering fraction is small ($\ll 50\%$), its effect on our analysis is minimal. In this case, it is immaterial whether the spot coverage is the same during the photometric and spectroscopic observations (as long as it is small during both).

E. Binarity

We only concern ourselves here with relatively binaries, where potential complications arise from both components appearing in the photometric and spectroscopic measurements. We examine three cases: equal-brightness binaries, binaries with slightly (500K) cooler secondaries, and binaries with much cooler and fainter secondaries. Secondaries much cooler (and correspondingly much fainter) than the primary will not affect our derived parameters for the primary. Considering the high binary fraction found by other investigators in low-mass PMS samples in different clusters, binarity may affect our sample as well. However,

given that only relatively close binaries can affect our analysis at all, and moreover that none of our targets are double-lined, the binary phase space that affects us is restricted to single-lined systems, and thus severely curtailed. In other words, we do not expect a large fraction of our targets to be binaries. We can safely ignore the issue of eclipsing systems, since they are very rare, and quite unlikely to affect our small sample.

For equal-brightness systems, i.e, equal T_{eff} and gravity (assuming coequality), our T_{eff} , gravity and A_V estimates will not be affected, since both components contribute similar spectra and photometric fluxes. However, the observed luminosity will be greater than that from any one component. In the worst-case scenario, we will overestimate luminosity by a factor of 2, and hence overestimate radius and mass by factors of $\sqrt{2}$ and 2 respectively.

Now consider secondaries cooler by $\sim 500\text{K}$ than the primary. First assume that both have the same radius. In that case, in analogy to the 500K cooler cool-spot case, we will infer a $T_{eff} \sim 200\text{K}$ lower than the primary's. Our gravity estimate will not be significantly affected even if the secondary's gravity is 0.5 dex smaller (in analogy with a low-gravity cool spot, discussed in Paper I). Our A_V estimates will also be only marginally affected, as in the cool spot case. However, the observed J magnitude will on average be similar to that from two stars, each cooler than the real primary by $\sim 200\text{K}$ (assuming one component is not occluding the other). The model spectra indicate that, for T_{eff} in the 3000-2500K range, a decrease in T_{eff} by 100K leads to J fainter by ~ 0.15 mag. The observed J -band flux in our case will then differ from the primary's by $(2 \times 0.15) - 2.5 \log(2)$, i.e., the system will appear ~ 0.35 mag brighter in J than the primary alone. We will thus overestimate the primary's luminosity by roughly 40%, and overestimate its radius and mass by about 20% and 40% respectively (very similar conclusions are reached if one uses I_C fluxes instead of J to calculate radius, mass and luminosity). Of course, if the cooler component has a smaller radius (as is likely for coeval objects), then we would be even less affected by its presence, since its flux contribution would be much lower.

F. Extinctions in GG Tau

One potential cause for concern is the difference in the extinctions we derive for GG Tau Ba and Bb; for Ba we find $A_V=0.29$ mag, and for Bb 1.76 mag. In their analysis of GG Tau, WGRS99 have inferred $A_V = 0.55$ mag for Ba, and 0.0 for Bb. Two questions may then be posed. First, is it plausible that Ba and Bb have visual extinctions differing by 1.5 mag, as we find? Second, how do we explain the difference between our and WGRS99's estimates?

We address the plausibility issue first. WGRS99 find an A_V of 0.72 mag for GG Tau Aa,

3.20 for Ab, and, as noted above, 0.55 mag for Ba and 0.0 for Bb. Thus, even their analysis indicates a substantial variation in extinction among the four components of GG Tau. The large difference in A_V that WGRS99 find between Aa and Ab is somewhat surprising, given that they are separated by only $0''.25$. It is possible, as WGRS99 suggest, that this arises from differences in the local distribution of circumstellar material around each star; whether this is actually the case, given that GG Tau A is an almost face-on system, remains an open question. At any rate, it seems very likely that there is at least a moderate amount of extinction towards both components of GG Tau A, and towards GG Tau Ba as well (as both WGRS99 and we find). The Taurus star-forming region is also known to be a heavily reddened one. Under the circumstances, our estimate of $A_V \sim 1.8$ seems unremarkable; it would perhaps be more surprising, given its environs and the observed A_V in the other 3 GG Tau members, if GG Tau Bb did not have any extinction at all. We further note that the separation between Ba and Bb is $1''.48$, much larger than between Aa and Ab; if, as WGRS99 find, even Aa and Ab can differ in A_V by ~ 2.5 mag, there is no a priori reason to discard our result of a smaller, 1.5 mag A_V difference between the much wider pair Ba and Bb. Finally, we point out that our errors in extinction are, on average, $\sim \pm 0.7$ mag⁵. Consequently, our A_V results are not incompatible with Ba and Bb actually being more similar to each other in extinction, than our quoted A_V values might at first suggest. We emphasize that we have accounted for such A_V uncertainties in our mass, radius and luminosity analysis, so our conclusions regarding the latter quantities are unaffected by our discussion here.

The second question is why our A_V estimate for Bb differs significantly from that of WGRS99. The answer lies in the difference in methodology used in the two studies. Our method has already been discussed in §3.1. Basically, our high-resolution spectral analysis allows us to first derive gravity and T_{eff} independent of extinction, through comparison with synthetic spectra (Paper I); we then adopt the intrinsic colors implied by the synthetic spectra (for the derived T_{eff} and $\log g$), and compare to the observed colors, to infer A_V . WGRS99, on the other hand, calculate A_V on the basis of spectral type considerations. For GG Tau Bb, they find a spectral type of M7 (slightly different from the more recent, and more accurate estimate of M7.5 by White & Basri 2002 and Luhman 1999). To derive A_V , they then use as a color template the M7 field dwarf VB8 (GJ 644C), which has $R_C - I_C = 2.41$ (Kirkpatrick & McCarthy 1994). The observed $R_C - I_C$ of GG Tau Bb, according

⁵Our estimated A_V error of ± 0.7 mag assumes an error of ~ 0.12 mag in observed $R_C - I_C$ (§3.3). This is accurate for our Upper Sco targets. For GG Tau Ba and Bb, the errors in observed R_C and I_C quoted by WGRS99 (whose photometry we use for GG Tau) implies an A_V error of ± 0.4 mag for Ba, and of ± 1 mag for Bb (calculated by adding in quadrature the other errors in our analysis, e.g., in determining T_{eff} and gravity; §3.2). This does not create any substantial difference in our conclusions: our A_V error for Ba is slightly less than 0.7 mag, and for Bb slightly more, so an average error of 0.7 mag for each is a good estimate.

to WGRS99, is 2.46. Using VB8 as a template then implies, through our eqn[1] (§3.1) for calculating extinction, an A_V of 0.24 mag for Bb, quite close to the $A_V = 0.0 \pm 0.24$ mag that WGRS99 quote⁶. Now, according to the latest T_{eff} scale for field M dwarfs (Leggett et al. 2000; see discussion in Paper I), an M7 dwarf should have $T_{eff} \lesssim 2500\text{K}$. Assuming $T_{eff} = 2500\text{K}$, a reasonable gravity of ~ 5.0 , and solar-metallicity, the synthetic spectra then predict an $R_C - I_C$ color of ~ 2.3 for VB8 (see Fig. 5). In other words, the predicted $R_C - I_C$ color of VB8, based on spectral type, is already quite close to the observed color; slightly lower T_{eff} , slightly higher gravity and/or metallicity effects are likely to account for any remaining difference. This line of reasoning shows that, *if* we adopted the WGRS99 method of using field dwarf colors as a template to calculate extinction in Bb, we would arrive at a very similar result (i.e., very low extinction) even using our synthetic photometry.

The real issue, therefore, is whether a field dwarf of the same spectral type accurately represents the intrinsic colors of GG Tau Bb. If PMS objects are $\sim 100\text{-}150\text{K}$ hotter than dwarfs of the same type (as suggested by WGRS99 themselves, as well as Luhman 1999), then GG Tau Bb (M7.5) should roughly have $T_{eff} \gtrsim 2500\text{K}$ (consistent with our derived T_{eff} of $\sim 2600\text{K}$; Paper I)⁷. Fig. 5 shows that, according to the synthetic spectra, PMS objects ($\log g \lesssim 4.0$) with $T_{eff} \gtrsim 2500\text{K}$ are bluer by >0.2 mag in $R_C - I_C$ than VB8; the latter thus seems to be an unreliable template for GG Tau Bb. Indeed, the same problem is evident, and in fact exacerbated, if we assign to Bb the T_{eff} that WGRS99 themselves find. The latter authors compare their observations to the BCAH98 evolutionary tracks to derive $T_{eff} \sim 2800\text{K}$ and age ~ 1.5 Myr for Bb. These *same* tracks, however, also state that an object with this T_{eff} and age should have an intrinsic $R_C - I_C \sim 2.0$ - i.e., much bluer than VB8 (see BCAH98; our synthetic spectra also suggest $R_C - I_C \sim 2.0$ for a PMS object at $\sim 2800\text{K}$, see Fig. 5). Even a field dwarf at 2800K has $R_C - I_C \sim 2.1$ (Fig. 5), considerably bluer than VB8. These considerations imply that by relying on spectral type, WGRS99 have ascribed intrinsic colors to GG Tau Bb that are too red, and thus underestimated its A_V .

⁶WGRS99 use 3 colors ($V - R_C$, $R_C - I_C$, $I_C - J$) to derive A_V , not $R_C - I_C$ alone. Consequently, their stated $A_V \approx 0 \pm 0.24$ mag is slightly (but not significantly) different from the $A_V \approx 0.24$ they would have found using $R_C - I_C$ alone. To facilitate comparison to our A_V results (derived from just $R_C - I_C$), we concentrate on $R_C - I_C$ in our present discussion.

⁷WGRS99 find a T_{eff} of $\sim 2800\text{K}$ for Bb, which is $\sim 300\text{K}$ hotter than an M7 dwarf according to the latest M dwarf T_{eff} scale (Leggett et al. 2000). WGRS99’s argument that PMS objects are $\sim 100\text{-}150\text{K}$ hotter than dwarfs of the same spectral type is in fact based on the older T_{eff} scale for dwarfs by Leggett et al. 1996; the older scale was $\sim 200\text{K}$ hotter than the new one. However, our T_{eff} of $\sim 2600\text{K}$ for Bb is indeed only $\sim 100\text{K}$ hotter than the new scale. That is, the difference between WGRS99’s value for Bb and the old M dwarf T_{eff} scale is the same as the difference between our value for Bb and new M dwarf scale - $\sim 100\text{K}$ in either case. These considerations are discussed in detail in Paper I.

Under the circumstances, one might ask why a similar discrepancy is *not* seen between our and WGRS99’s values for A_V in GG Tau Ba: we find a visual extinction of 0.29 mag, while WGRS99 find an almost identical (within the errors) value of 0.55 mag⁸. The answer once again lies in spectral typing uncertainties. WGRS99 derive a spectral type of M5 for Ba, and thus compare its colors to those of M5 dwarfs from the literature. Specifically, they use M5 dwarf colors from Kirkpatrick & McCarthy 1994, who quote $R_C - I_C = 1.89$, calculated by averaging the colors of the two M5 dwarfs Gl 51 and GJ 1057⁹. However, the spectral type of Ba has been pushed down in the intervening years; Luhman 1999 found M5.5 through a more careful analysis, and the latest estimate is M6, by White & Basri 2002. WGRS99 have therefore compared Ba to a field dwarf with an earlier spectral type, and thus bluer in $R_C - I_C$, than appropriate within their scheme for deriving A_V . At the same time, as we have noted above in our discussion of GG Tau Bb, dwarfs of a given spectral type seem to be redder in the optical than PMS objects of the same type: higher gravity alone, at a fixed T_{eff} , leads to redder $R_C - I_C$ (Fig. 5); it may also be that PMS objects are systematically somewhat hotter than dwarfs of the same type (Luhman 1999; our results in Paper I generally agree with this view), which exacerbates the color difference. In general, this causes an underestimation of A_V in the WGRS99 scheme (as was the case for Bb). In the case of Ba, however, WGRS99’s use of a dwarf template that is *earlier* in type than Ba offsets this effect, producing an A_V quite similar to ours. Note that if WGRS99 had used an M6 field dwarf as template, as dictated by the newest spectral type for Ba, they would indeed have found a substantially lower A_V than we do, analogous to the situation for Bb. For instance, Kirkpatrick & McCarthy 1994 quote an average $R_C - I_C$ of 2.17 mag for M6 dwarfs. Using this, WGRS99 would have found no extinction at all. In fact, strictly speaking, using the M6 dwarf color yields an unphysical negative extinction ($A_V = -1$) for Ba (which has $R_C - I_C = 1.97$ according to WGRS99). This is further evidence that dwarf optical colors are intrinsically redder than PMS ones at these spectral types. A detailed discussion of color differences between dwarf, giant and PMS regimes can be found in Luhman 1999.

The above discussion clearly illustrates the problems, alluded to in Appendix A, of using spectral type considerations for PMS analysis. Our methodology, in Paper I and here, avoids these difficulties by making no a priori assumptions about intrinsic PMS colors based on spectral typing: T_{eff} and gravity are first inferred in an extinction-independent fashion,

⁸As in Bb, the WGRS99 A_V for Ba is from a 3-color analysis, using template dwarf colors from Kirkpatrick & McCarthy 1994; $R_C - I_C$ alone would imply $A_V=0.39$ in the WGRS99 scheme, even closer to our value.

⁹One of these, GL 51, has been analysed by Leggett et al. 2000, and found to have a T_{eff} of 2900K; it is plotted in Fig. 5 ($T_{eff} = 2900\text{K}$, $R_C - I_C = 1.92$) along with another M5 dwarf analysed by the same authors, GJ 1029 ($T_{eff} = 2900\text{K}$, $R_C - I_C = 1.93$).

and the extinctions then derived self-consistently, by adopting the intrinsic colors implied by the same synthetic spectra that are used for the T_{eff} and gravity analysis.

REFERENCES

- Allard,F., Hauschildt,P.H., Schwenke,D., 2000, ApJ, 540, 1005
- Ardila,D., Martín,E.L., Basri,G., 2000, AJ, 120, 479 [AMB00]
- Baraffe,I., Chabrier,G., Barman,T.S., Allard,F., Hauschildt,P.H., 2003, A&A, 406, 1001
- Baraffe,I., Chabrier,G., Allard,F., Hauschildt,P.H., 2002, A&A, 382, 563 [BCAH02]
- Baraffe,I., Chabrier,G., Allard,F., Hauschildt,P.H., 1998, A&A, 337, 403 [BCAH98]
- Basri,G., *What is a ‘Planet’?*, 2003, Mercury, vol. 32, 6, p.27
- Bate,M.R., Bonnell,I.A., Bromm,V., 2002, MNRAS, 332, L65
- Boss,A.P., 2001, ApJ, 551, L167
- Briceno,C., Luhman,K., Hartmann,L., Stauffer,J., Kirkpatrick,D., 2002, ApJ, 580, 317
- Burrows,A., Sudarsky,D., Hubbard,W.B., 2003, ApJ, 594, 545
- Burrows,A., Liebert,J., 1993, Rev. Mod. Phys., 65, 301
- Carpenter,J.M., 2001, AJ, 121, 2851
- Chabrier,G., Baraffe,I., Allard,F., Hauschildt,P.H., 2000, ApJ, 542, 464 [CBAH00]
- Charbonneau,D., Brown,T.M., Noyes,R.W., Gilliland,R.L., 2002, ApJ, 568, 377
- Close,L.M., Potter,D., Brandner,W., Lloyd-Hart,M., Liebert,J., Burrows,A., Siegler,N., 2002, ApJ, 566, 1095
- D’Alessio,P., Calvet,N., Hartmann,L., Lizano,S., Cantó,J., 1999, ApJ, 527, 893
- D’Alessio,P., Calvet,N. & Hartmann,L., 2001, ApJ, 553, 321
- Fernández,M. & Comerón,F., 2001, A&A, 380, 264
- Guilloteau,S., Dutrey,A., Simon,M., 1999, A&A, 348, 570
- Gullbring,E., Hartmann,L.W., Briceño,C., Calvet,N., 1998, ApJ, 492, 323
- Hartigan,P., Strom,K.M., Strom,S.E., 1994, ApJ, 427, 961
- Hartmann,L., 2003, ApJ, 585, 398

- Herbig,G.H., 1998, ApJ, 497, 736
- Jayawardhana,R., Mohanty,S., Basri,G. 2002, ApJ, 578, L141
- Jayawardhana,R., Mohanty,S., Basri,G. 2003, ApJ, 592, 282
- Jayawardhana,R., Ardila,D., Stelzer,B., Haisch,K.E.,Jr., 2003, AJ, 126, 1515
- Kenyon,S.J., Dobrzycka,D., Hartmann,L., 1994, AJ, 108, 1872
- Kirkpatrick,J.D. et al., 1999, ApJ, 519, 802
- Kirkpatrick,J.D., Henry,T.J., Irwin,M.J., 1997, AJ, 113, 1421
- Kirkpatrick,J.D., Henry,T.J., Simons,D.A., 1995, AJ, 109, 797
- Kirkpatrick,J.D., McCarthy,D.W.,Jr., 1994, AJ, 107, 333
- Kirkpatrick,J.D., Henry,T.J., McCarthy,D.W., 1991, ApJS, 77, 417
- Klein,R., Apai,D., Pascucci,I., Henning,Th., Waters,L.B.F.M., ApJ, 593, L57
- Lane,B.F., Zapatero Osorio,M.R., Britton,M.C., Martín,E.L., Kulkarni,S.R., 2001, ApJ, 560, 390
- Leggett,S.K., Allard,F., Geballe,T.R., Hauschildt,P.H., Schweitzer,A., 2001, ApJ, 548, 908
- Leggett,S.K., Allard,F., Dahn,C., Hauschildt,P.H., Kerr,T.H., Rayner,J., 2000, ApJ, 535, 965
- Leggett,S.K., Allard,F., Berriman,G., Dahn,C.C., Hauschildt,P.H., 1996, ApJS, 104, 117
- Leggett,S.K., 1992, ApJS, 82, 351
- Lucas,P.W., Roche, P.F. 2000, MNRAS, 314, 858
- Luhman,K.L., 1999, ApJ, 525, 466
- Mohanty,S., Jayawardhana,R., Barrado y Navascués, D., 2003, ApJ, 593, L109
- Mohanty,S., Basri,G., Jayawardhana,R., Allard,F., Hauschildt,P., Ardila,D., 2003, ApJ, submitted [Paper I]
- Montalban,J., D’Antona,F., Kupka,F., Heiter,U., 2003, A&A, submitted
- Najita,J.R., Tiede,G.P., Carr,J.S. 2000, ApJ, 541, 977

- Barrado y Navascués,D., Mohanty,S. & Jayawardhana,R., 2003, ApJ, accepted
- Padgett,D., Brandner,W., Stapelfeldt,K., Strom,S., Terebey,S., Koerner,D., 1999, AJ, 117, 1490
- Padoan,P. & Nordlund,Å., 2002, ApJ, 576, 870
- Potter,D., Martín,E.L., Cushing,M.C., Baudoz,P., Brandner,W., Guyon,O., Neuhäuser,R., 2002, ApJ, 567, L133
- Preibisch,T., Brown,A.G.A., Bridges,T., Guenther,E., Zinnecker,H., 2002, AJ, 124, 404
- Reipurth,B. & Clarke,C., AJ, 122, 432.
- Ribas,I., 2003, A&A, 398, 239
- Schlegel,D.J., Finkbeiner,D.P., Davis,M., 1998, ApJ, 500, 525
- Stassun,K.G., Mathieu,R.D., Vaz,L.P.R., Stroud,N., Vrba,F.J., 2003, ApJ, accepted
- Torres,G., & Ribas,I., 2002, ApJ, 567, 1140
- White,R.J. & Basri,G., 2002, ApJ, accepted
- White,R.J., Ghez,A.M., Reid,I.N., Schultz,G., 1999, ApJ, 520, 811 [WGRS99]
- Zapatero Osorio,M.R., Béjar,V.J.S., Martín,E.L., Rebolo,R., Barrado y Navascués,D., Bailer-Jones, C.A.L., Mundt,R. 2000, Science, 290, 103

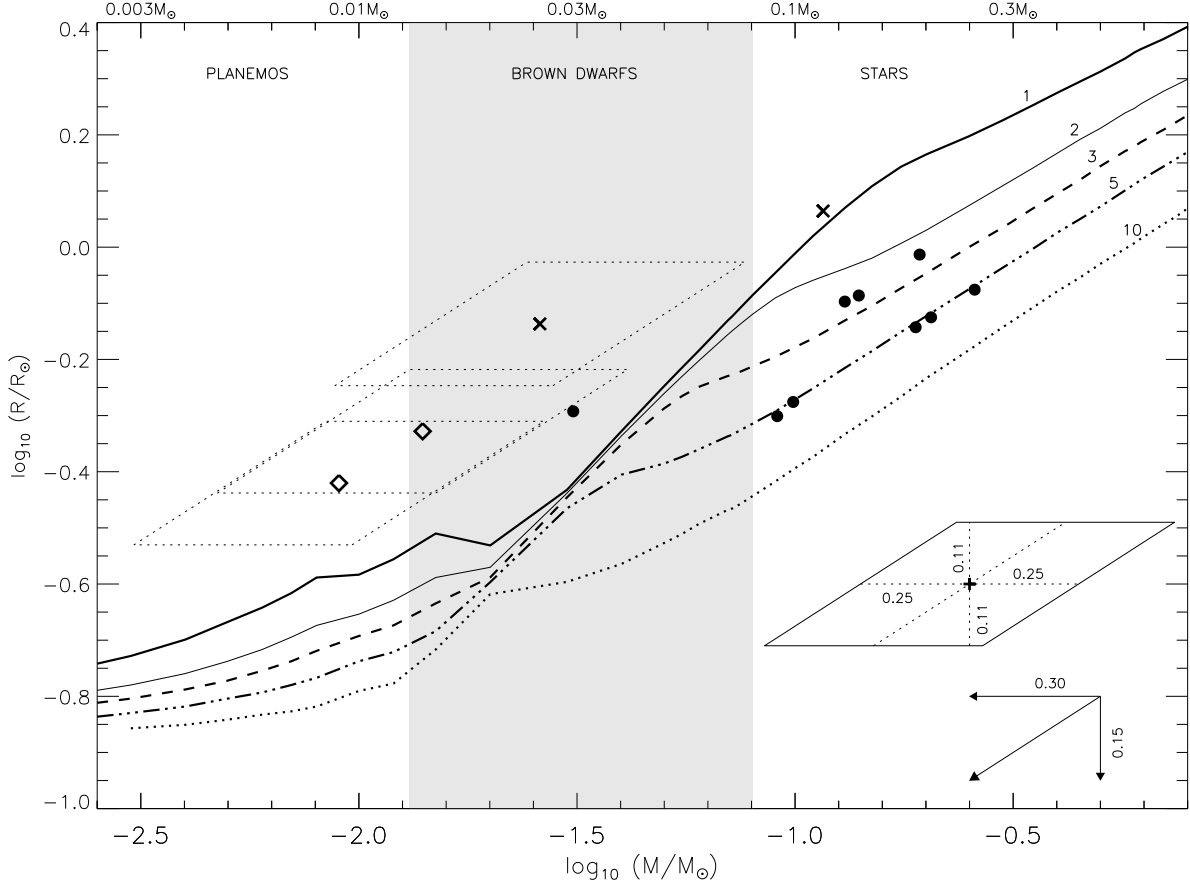


Fig. 1.— Our derived radii and masses (based on J fluxes; see §3.1), plotted against the Lyon98/00 isochrones (track ages denoted in Myr units). The central grey region delineates the brown dwarf regime, while the regions to the left and right of it indicate the planemo and stellar regimes respectively. Diamonds represent the two Upper Sco objects near the planemo boundary (USco 128 & 130); filled circles indicate all other Upper Sco targets. The crosses denote GG Tau Ba and Bb (Ba has the larger mass). Error bars are indicated: the vertical line represents ± 0.11 dex errors in radius; the horizontal line represents the error in mass at fixed radius, due to our ± 0.25 dex uncertainty in gravity. At a fixed $\log g$, changing radius makes an object move diagonally in the mass-radius plane (since our mass depends on radius), as shown by the diagonal lines superimposed on the error bars. For the 3 targets with the largest offset from the tracks, the error boundaries are also superimposed on our data points to clearly illustrate their disagreement with the tracks. The horizontal and vertical arrows at the bottom right show, respectively, the shift in inferred mass and radius that would result if any object were actually an equal-mass binary; the diagonal arrow indicates the combined shift. Masses $\gtrsim 0.03 M_{\odot}$ agree with the Lyon radius predictions for the expected ages, while lower masses have significantly larger radii than predicted. See §4.1.

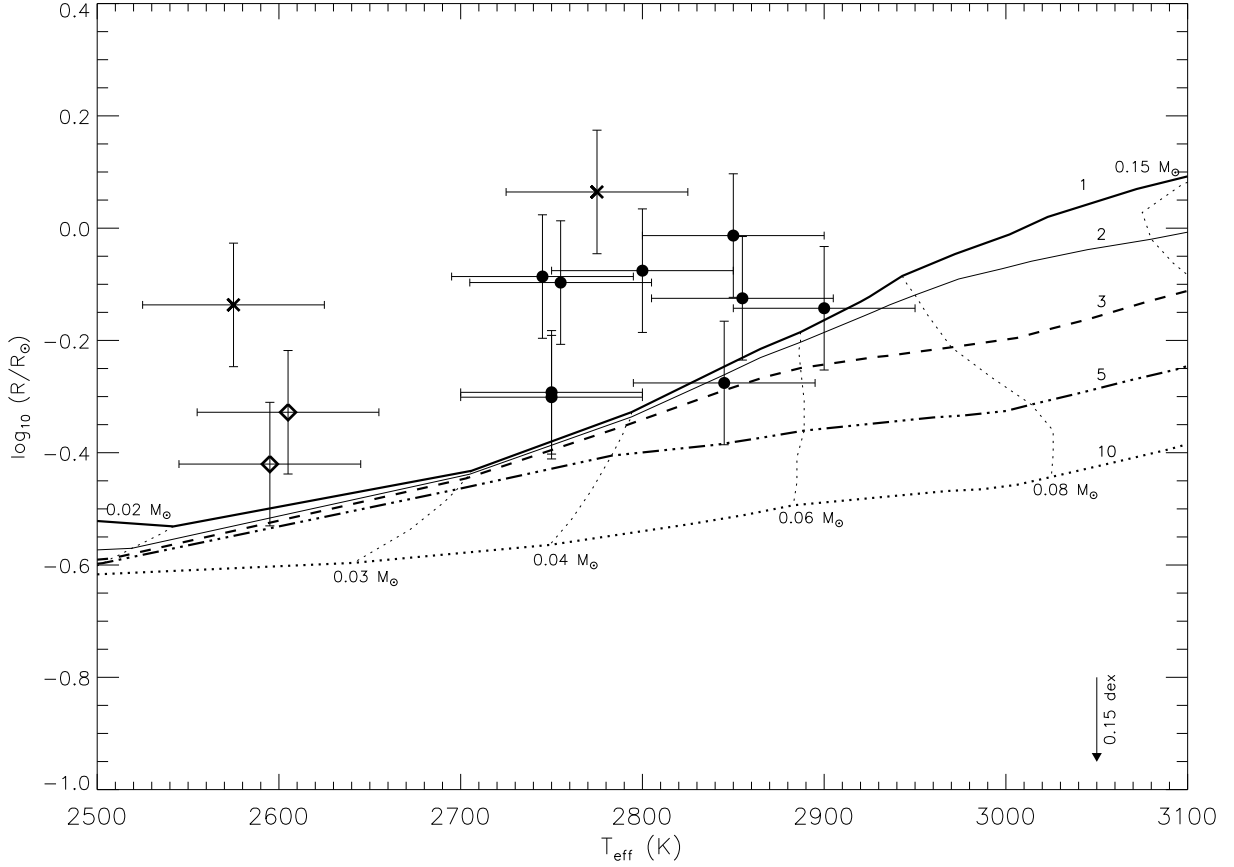


Fig. 2.— Our derived T_{eff} and radii (latter based on J fluxes), versus the Lyon98/00 predictions. All symbols are the same as in Fig. 1. The theoretical evolutionary paths for various masses are also plotted (dotted lines); note that these are *not* necessarily the masses we derive for our targets. Error bars are $\pm 50\text{K}$ in T_{eff} , and ± 0.11 dex in radius. The vertical arrow at the bottom right indicates the shift in inferred radius that would result if any target were an equal mass binary. While all the objects appear displaced from the Lyon isochrones, the reasons for this vary: the 3 coolest objects (GG Tau Bb and USco 128 & 130) are offset because their derived radii are much larger than predicted, while the other, hotter targets are offset because their inferred temperatures are much lower than predicted (as apparent by comparing to Figs. 1 and 3; see also §4.2).

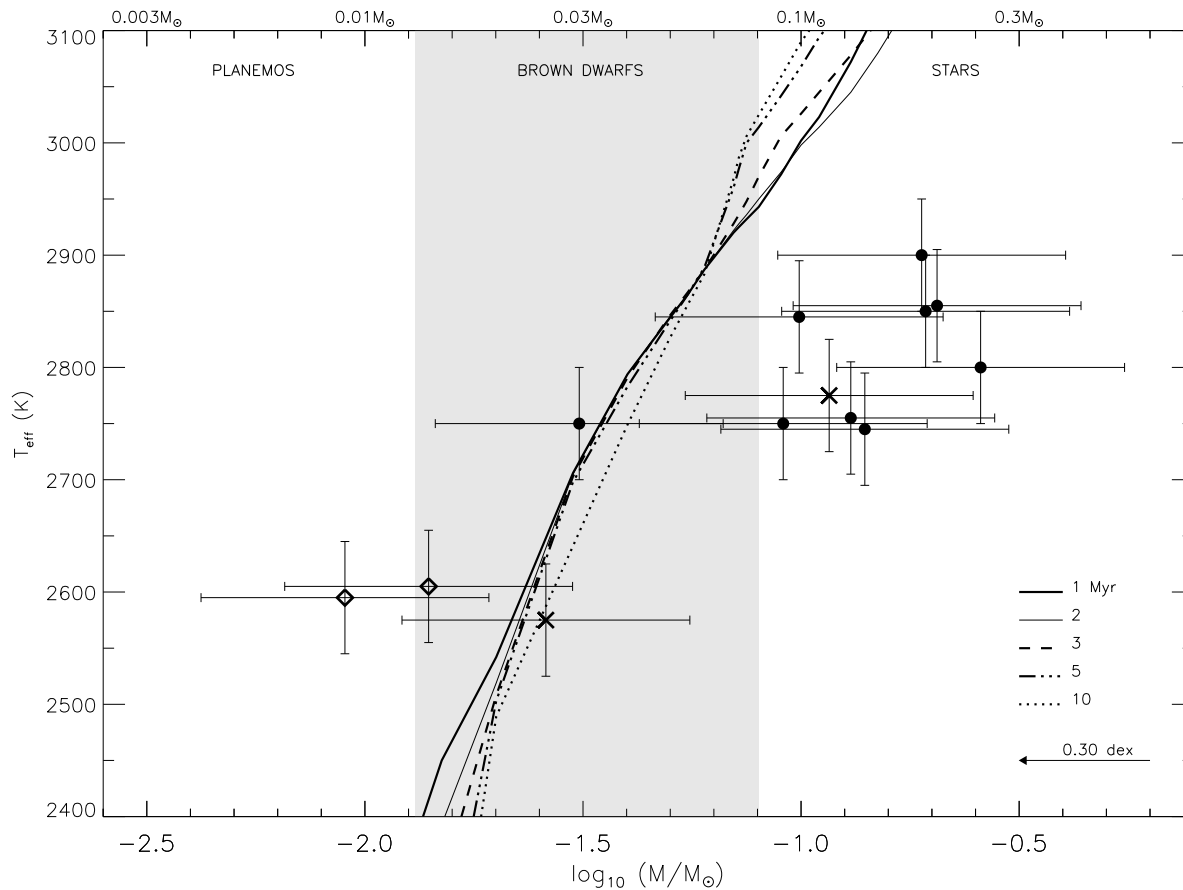


Fig. 3.— Our derived T_{eff} and masses (latter based on J fluxes), versus the Lyon98/00 predictions. All symbols are the same as in Fig. 1. Error bars are $\pm 50\text{K}$ in T_{eff} , and ± 0.33 dex in mass. The arrow at the bottom right indicates the shift in inferred mass that would result if any object were an equal mass binary. Our inferred T_{eff} -mass relationship appears shallower than predicted: the two lowest mass targets appear hotter than expected; the two intermediate masses in the brown dwarf regime agree quite well with the Lyon T_{eff} , and the more massive targets all appear much cooler than predicted for their mass. See §4.2.

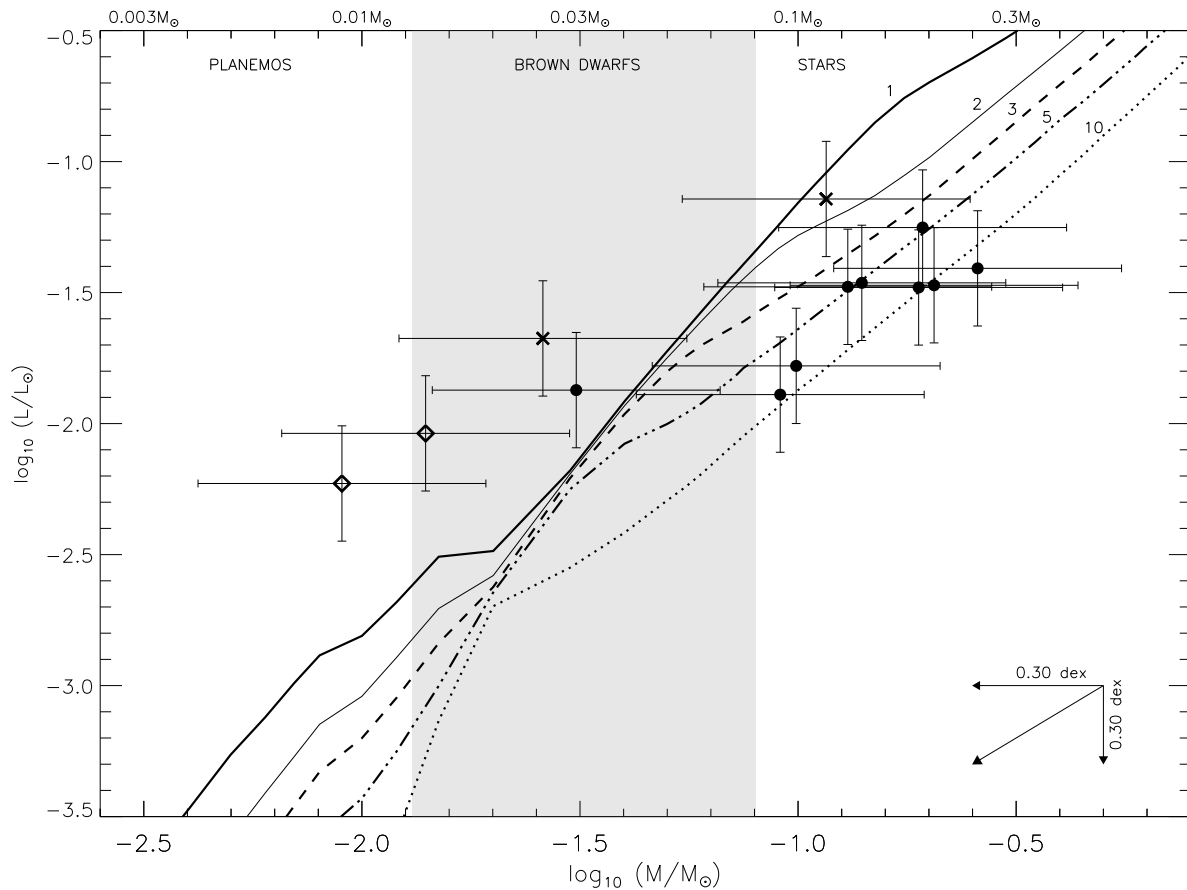


Fig. 4.— Our derived masses and luminosities (based on J fluxes), versus the Lyon98/00 predictions. All symbols are the same as in Fig. 1. Errors are ± 0.33 dex in mass and ± 0.22 dex in \mathcal{L}_{bol} . The horizontal and vertical arrows at the bottom right indicate, respectively, the shift in inferred luminosity and mass that would result if any object were an equal mass binary; the diagonal arrow indicates the combined shift. See §4.3.

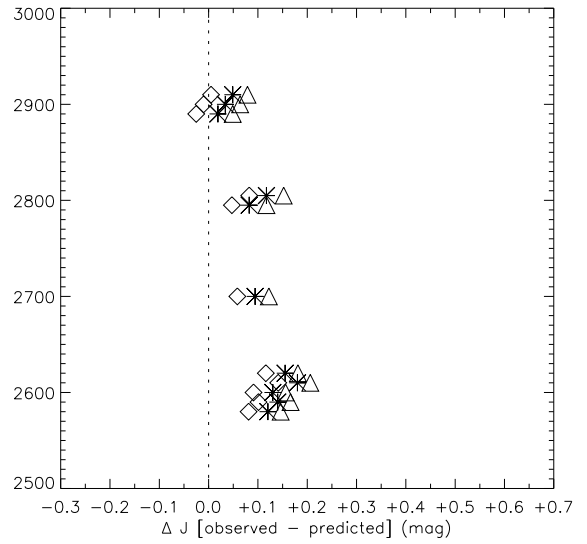
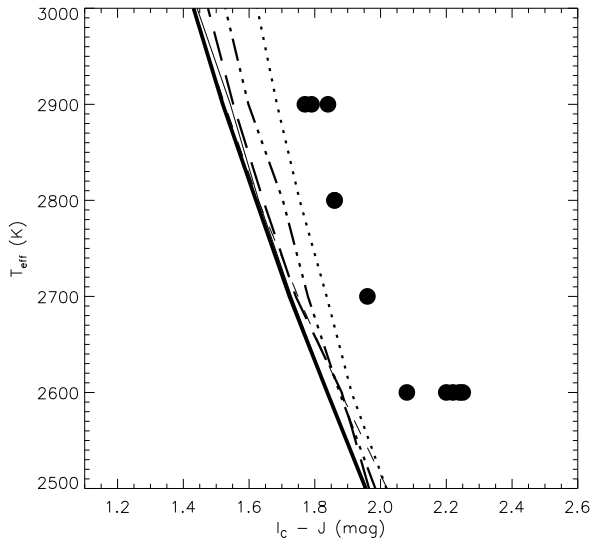
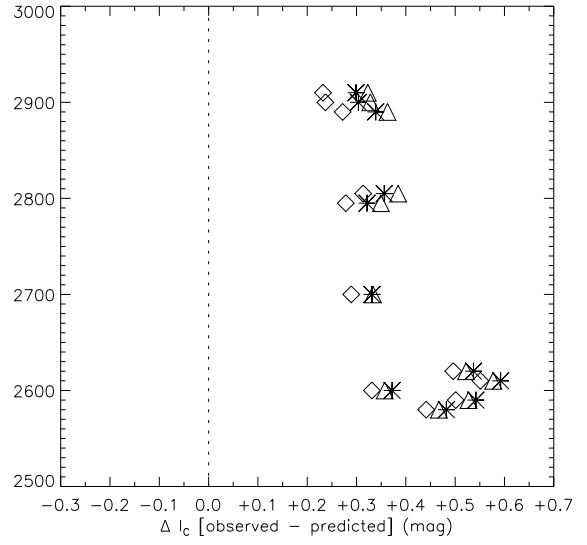
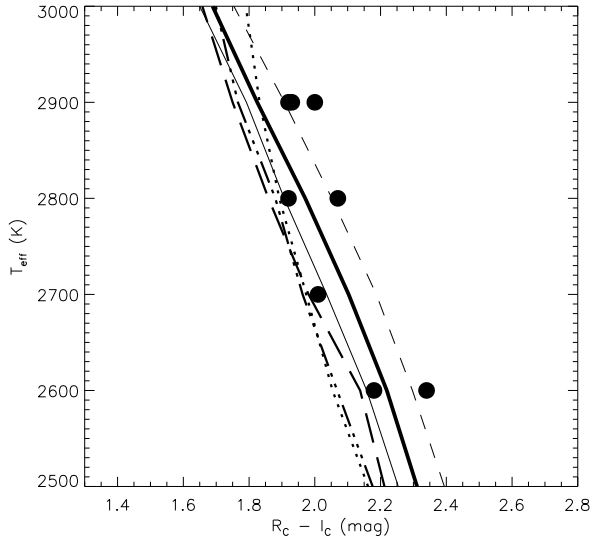
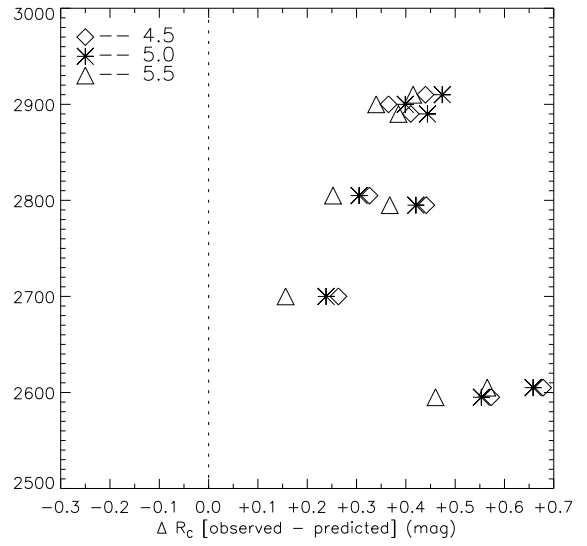
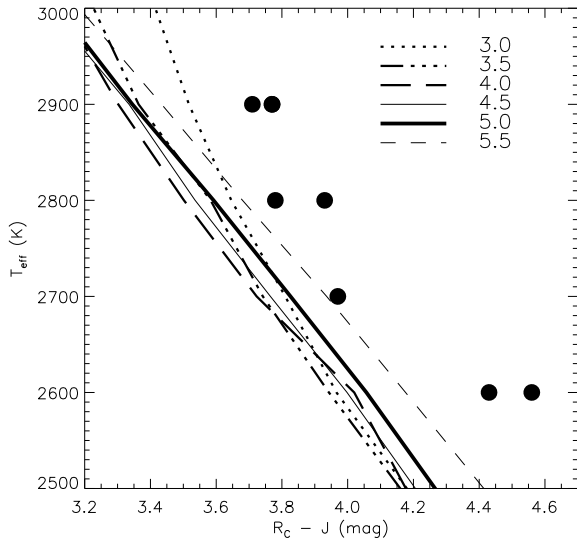


Fig. 5.— Derived T_{eff} -photometry relationships for field dwarfs, compared to synthetic spectra predictions for various gravities. Data from Leggett et al. (2000). The expected gravity of field dwarfs is $\log g \approx 4.5\text{--}5.5$. *Left column:* T_{eff} -color relationship, for various colors: $R_C\text{--}J$ (top), $R_C\text{--}I_C$ (middle) and $I_C\text{--}J$ (bottom). The synthetic spectra predictions are too blue in $R_C\text{--}J$ and $I_C\text{--}J$, but match the observations quite well in $R_C\text{--}I_C$. *Right column:* T_{eff} -flux relationship, for various photometric bands: R_C (top), I_C (middle) and J (bottom). In each panel, we show the observed flux minus the predicted flux (corrected for known distance) at the derived T_{eff} , for three gravities covering the expected range of dwarf gravities (triangle, asterisk and diamond denote $\log g = 4.5, 5.0$ and 5.5 respectively). If the synthetic flux matched the observations exactly for some gravity at a given T_{eff} , the corresponding data point would lie on the vertical dotted line (which corresponds to zero offset). We see that the model spectra are overluminous, compared to the observations, in both R_C and I_C , but perform quite well (errors $\lesssim 0.2$ mag) in J . See Appendix A. These plots provide the rationale for our choosing $R_C\text{--}I_C$ colors to derive extinctions for our targets, and J -band photometry to derive radii, masses and luminosities.

Table 1. Temperatures, Gravities, Photometry & Extinctions

name	SpT ^a	T _{eff} ^b (K)	log <i>g</i> ^b	R _C ^c (mag)	I _C ^c (mag)	J ^d (mag)	A _V ^e (mag)	A _{I_C} ^e (mag)	A _J ^e (mag)
USco 55	M5.5	2800	4.00	16.70	14.58	12.46	1.24	0.74	0.35
USco 66	M6	2900	4.00	17.03	14.85	12.91	2.05	1.23	0.58
USco 53	M5	2850	3.75	16.76	14.54	12.29	1.90	1.14	0.54
USco 75	M6	2850	4.00	17.25	15.08	12.78	1.71	1.03	0.48
USco 67	M5.5	2750	3.75	16.99	14.87	12.54	0.95	0.57	0.27
USco 100	M7	2750	3.75	17.95	15.62	12.84	1.95	1.17	0.55
USco 109	M6	2750	4.00	18.21	16.06	13.61	1.10	0.66	0.31
USco 112	M5.5	2850	4.00	18.22	16.14	13.46	1.29	0.77	0.36
USco 104	M5	2750	3.50	17.76	15.68	13.48	0.76	0.46	0.21
USco 130	M7.5	2600	3.25	19.91	17.45	14.20	1.90	1.14	0.54
USco 128	M7	2600	3.25	19.38	17.09	14.40	1.10	0.66	0.31
GGTau Ba	M6	2775	3.375	15.36	13.39	11.48	0.29	0.17	0.08
GGTau Bb	M7.5	2575	3.125	18.01	15.55	13.16	1.76	1.06	0.50

^aSpectral Types for Upper Sco objects from AMB00, and for GG Tau Ba and Bb from White & Basri 2002.

^bT_{eff} and gravity derived in Paper I; errors $\approx \pm 50\text{K}$ and ± 0.25 dex respectively; derived assuming solar metallicity ([M/H]=0).

^cObserved R_C and I_C, uncorrected for extinction; taken from AMB00 for Upper Sco objects, and from WGRS99 for GG Tau Ba and Bb.

^dObserved J, uncorrected for extinction; taken from 2MASS for Upper Sco objects, and from WGRS99 for GG Tau Ba and Bb.

^eExtinctions from comparing the observed R_C – I_C colors to synthetic ones (for the derived T_{eff} and log *g*); error in A_V $\approx \pm 0.7$ mag. A_{I_C} = 0.60 A_V; error $\approx \pm 0.42$ mag. A_J = 0.28 A_V; error $\approx \pm 0.20$ mag.

Table 2. Radii, Masses & Luminosities

name	T_{eff}	$\log g$	I_C			J		
			$\frac{M}{M_\odot}$	$\frac{R}{R_\odot}$	$\frac{\mathcal{L}_{bol}}{L_\odot}$	$\frac{M}{M_\odot}$	$\frac{R}{R_\odot}$	$\frac{\mathcal{L}_{bol}}{L_\odot}$
USco 55	2800	4.00	0.24	0.81	0.036	0.26	0.84	0.039
USco 66	2900	4.00	0.24	0.81	0.042	0.19	0.72	0.033
USco 53	2850	3.75	0.19	0.96	0.055	0.19	0.97	0.056
USco 75	2850	4.00	0.18	0.70	0.029	0.21	0.75	0.033
USco 67	2750	3.75	0.10	0.70	0.025	0.14	0.81	0.034
USco 100	2750	3.75	0.088	0.66	0.022	0.14	0.81	0.034
USco 109	2750	4.00	0.063	0.41	0.009	0.091	0.50	0.013
USco 112	2850	4.00	0.053	0.38	0.009	0.099	0.52	0.016
USco 104	2750	3.50	0.025	0.47	0.011	0.031	0.52	0.014
USco 130	2600	3.25	0.007	0.33	0.004	0.014	0.47	0.009
USco 128	2600	3.25	0.006	0.31	0.004	0.009	0.38	0.006
GGTau Ba	2775	3.375	0.11	1.12	0.067	0.12	1.16	0.072
GGTau Bb	2575	3.125	0.028	0.75	0.022	0.026	0.73	0.021

Note. — Mass, radius and bolometric luminosity derived in this paper. The first set of values is derived using I_C fluxes, the second set using J . The internal stochastic errors in each are of order factor of 2 in mass, 30% in radius, and 65% in luminosity. All quantities are derived assuming solar metallicity. There is a systematic offset between the I_C - and J -derived values, with the latter generally being somewhat higher. Objects within a cluster (Upper Sco or Taurus) are listed in order of decreasing I_C -band mass; the ordering of objects by J -band mass is generally the same. The few most massive and/or most luminous USco objects may be spectroscopic binaries. Note that in Figs. 2–5, we have plotted the logarithm of mass, radius and luminosity; this table lists the linear values.